To the Graduate Council:

I am submitting herewith a thesis written by Khaled Meftah "Ignition and Combustion Phenomena of Laser-Ignited Aluminum Agglomerates at Elevated Pressures." I have examined the final copy of this thesis for form and content and recommend that it will be accepted in partial fulfillment of the requirements for the degree of Master of Science, with a major in Mechanical Engineering.

Ke Nguyen, Major Professor

We have read this thesis
and recommend its acceptance:

Accepted for the Council :

Associate Vice Chancellor
and Dean of The Graduate School

STATEMENT OF PERMISSION TO USE

In presenting this thesis in partial fulfillment of the requirements for a Master's degree at the University of Tennessee, Knoxville, I agree that the library shall make it available to borrowers under rules of the library. Brief quotations from this thesis are allowable without special permission, provided that accurate acknowledgement of the source is made.

Permission for extensive quotation from or reproduction of this thesis may be granted by my major professor, or in his absence, by the Head of Interlibrary Services when, in the opinion of either, the proposed use of the material is for scholarly purposes. Any copying or use of the material in the thesis for financial gain shall not be allowed without my written permission.

Signature KHALED Asfal

Date May 1st 1992

IGNITION AND COMBUSTION PHENOMENA OF LASER-IGNITED ALUMINUM AGGLOMERATES AT ELEVATED PRESSURES

A Thesis

Presented for the

Master of Science

Degree

The University of Tennessee, Knoxville

Khaled Meftah

May 1992

ACKNOWLEDGMENTS

I would like to express my sincere thanks to my advisor, Professor Ke Nguyen for his guidance, advice and patience during the course of this research. I would also like to thank Dr. Roger Parsons and Dr. Jeffrey W. Hodgson, who served on my graduate committee.

I hereby acknowledge the National Science Foundation for their invaluable research funding.

ABSTRACT

An experimental investigation of the ignition and combustion phenomena of laser-ignited aluminum agglomerates at elevated pressures is presented. Aluminum agglomerates of nominal diameter of 535 μm were ignited by a focused CO_2 laser pulse in a quiescent environment of O_2/N_2 (20/80) and at different ambient pressures ranging between 0.1 and 4.3 MPa. A two-color pyrometer and a broad band radiometer were employed to measure the surface temperature and the radiation emitted by the burning aluminum agglomerate, respectively. From the outputs of the two-color pyrometer and the broad band radiometer, the ignition temperature, the ignition delay time and the burning time were obtained. A high-speed camera was utilized to observe the phenomenological events during the burning of the aluminum agglomerate, and also to correlate with the results obtained from the pyrometer and radiometer.

In the range of pressures (0.1 to 4.3 MPa) investigated in the present study, aluminum agglomerates burn primarily in the vapor phase, characterized by a detached flame surrounding the burning droplets. At pressures below 2.2 MPa, the burning time was found to decrease with increasing ambient pressure. At high pressures (>2.2 MPa) the burning time is not sensitive to the ambient pressure. As the pressure increases, the flame moves closer to the aluminum droplet surface. In this study, the ignition of aluminum agglomerates occurs in the neighborhood of the melting temperature of the

aluminum oxide (2315 K) which indicates that the break-off of the aluminum oxide layer is the mechanism of aluminum ignition.

Qualitative studies of flame structure from high-speed camera showed that the flame, surrounding the aluminum burning droplet, consists of three different zones: a luminous white zone surrounded by a green thick envelope (AlO) which is in turn adjoined by a thin blue-violet zone. The luminosity of the inner zone increases with increasing pressure.

TABLE OF CONTENTS

LIST OF TABLES

TABLE PAGE

LIST OF FIGURES

FIGURE PAGE

FIGURE PAGE

CHAPTER 1
INTRODUCTION

Aluminum has been used extensively either as an additive in solid propellants or as a component for slurry fuels in air-breathing propulsion systems. Because of the high flame temperature (3800 K), aluminum powder when used as additive in solid propellant, can react with certain products of the propellant such as water and carbon dioxide to increase the gas temperature resulting in an increase in the specific impulse of rocket motors [1]. Since aluminum has a high volumetric heating value, its slurry fuels can substantially increase the range and velocity of aircraft equipped with volume limited air-breathing propulsion systems.

In general, metals such as aluminum and boron offer several advantages such as high energy content (Table 1.1), and unlike hydrocarbon fuels, metals release great energy due to their high flame temperatures. In spite of these advantages, metal combustion can also have detrimental effects on the burning process. For example, during the burning process in solid propellants, the fine metal powders can coalesce into a large agglomerate, resulting in longer burning times; and thus the impulse of the rocket motor might fall below that of a non-metalized propellants. In addition, the formation of the condensed oxide results in a two-phase flow which significantly decreases the nozzle thrust efficiency [1,2].

Previous studies [3-5] have shown that the burning of slurry

Table 1.1 Heating Values of Various Fuels [20]

Fuel	Gravimetric Heating Value cal/g	Volumetric Heating Value cal/cm^3
JP5	10,150	8,230
Shelldyne-H	9,860	10,000
Carbon	7,830	17,700
Aluminum	7,420	20,000
(CH2)n	10,400	9,600
Boron	13,800	32,200
Magnesium	5,910	10,300

fuel droplet occurs in two distinct stages. In the first stage, the liquid carrier evaporates and burns, leaving behind very fine solid particles that group together to form a porous agglomerate. In the second stage, this agglomerate heats up, ignites and burns. Because the combustor's residence time ranges from 20 to 100 ms, if the burning is not completed during that time, a dramatic decrease of the combustor efficiency can occur.

The combustion of metals depends solely on their physical and chemical properties such as: oxide melting temperature, boiling temperature of the metal, heat of reaction and flame temperature. One attraction of choosing aluminum over other metals is that like hydrocarbons, aluminum burns mainly in the vapor phase. Because the flame temperature is nearly equal to the boiling temperature of aluminum oxide (3800 K), aluminum vaporizes quickly which in turn accelerates the combustion rate.

Even though aluminum offers several advantages over other metals, its ignition and combustion represent some complexities. Because of the protective oxide layer formed around the heated particle, aluminum does not easily ignite. This oxide layer acts as a barrier to slow down the transport of the oxidants to the aluminum surface [2]. In addition to the agglomeration problem mentioned above, the accumulation of the vapor oxide on the droplet surface complicates the burning process, especially during the later burning stage where spinning, jetting and fragmentation are observed. Recognizing these problems, extensive studies, both experimental

and theoretical, have focused on the different characteristics of the combustion of aluminum particles.

These experimental studies have investigated the different effects of the environmental conditions on the ignition and combustion mechanisms of single aluminum particles. A number of techniques have been used to carry out these investigations. These techniques include the use of flat flame burners, laser pulses and pressurized bomb vessels. From these studies, as it will be shown later in chapter 2, the ignition and combustion of aluminum depend on different controlling parameters. For example, the ignition delay time is strongly affected by the ambient gas temperature. On the other hand, the oxygen concentration, water vapor content and the nature of the diluted gas (argon, nitrogen, carbon monoxide) affect the particles' burning mechanism which includes flame structure, oxide accumulation, fragmentation, jetting and spinning.

Although extensive research has been devoted to study the ignition and combustion of aluminum particles, the ignition and combustion of aluminum droplet slurries have been addressed only recently by Turns and Wong who conducted experimental and theoretical investigations on the ignition and combustion of aluminum droplet slurries.These studies will be discussed in chapter two.

The ignition and combustion of aluminum agglomerates at high pressure has not yet been addressed even though it represents a major issue in practical combustors where the operating pressure ranges between 0.1 and 2 MPa. Therefore, the objective of the pres-

ent investigation is :

1. To study the influence of the ambient pressure on the ignition delay time and total burning time of aluminum agglomerate
2. To study the flame structure as a function of the ambient pressure
3. To delineate the differences, if any, between the combustion of aluminum particles and aluminum agglomerates.

In the present study, probe-supported aluminum agglomerates were mounted in a high pressure combustion chamber, and ignited using a focused CO_2 laser pulse. Use of CO_2 laser ignition technique offers several advantages over other previously employed techniques. For example, the use of CO_2 laser pulse permits the separation of the heat source from the oxidizing gases. Furthermore, the ignition of aluminum agglomerates in the combustion chamber while at rest helps to vary the gas compositions and the ambient pressure; and also the flame structure can be easily observed and analyzed using a high-speed camera. Since the air-breathing propulsion system uses air as the oxidant, this study was restricted to environments of 20% oxygen mole fraction and 80% nitrogen. The pressure was varied from 0.1 to 4.3 MPa.

A two-color pyrometer was used to measure the surface temperature of aluminum agglomerate, whereas a broad band radiometer was employed to determine the total burning time of the agglomerate. To study the combustion phenomenon of the aluminum agglomerate, a high-speed motion picture camera was used to record the

combustion event. In this study, the ignition point is defined as the point at which the flame first appears. Therefore, the ignition delay time is the time elapsed between the beginning of the laser irradiation and the ignition point. The burning time is defined as the time elapsed between the ignition point and the instance at which no more oxide vapor is observed.

A literature survey of previous investigations on the ignition and combustion of both aluminum particles and aluminum agglomerates is given in chapter 2. Chapter 3 presents the experimental apparatus and procedures. The discussion and results are presented in chapter 4. Finally, conclusions and suggestions for future study are outlined in chapter 5.

CHAPTER 2
LITERATURE SEARCH

This chapter presents an overview of previous investigations on the ignition and combustion of both aluminum particles and aluminum agglomerates. In section 2.1, a review of the studies on the ignition and combustion of single aluminum particles is presented. In section 2.2, studies on the ignition and combustion of aluminum agglomerates are reviewed.

2.1 IGNITION AND COMBUSTION OF SINGLE ALUMINUM PARTICLES

Friedman and Macek [6] investigated the effect of oxygen concentration, ambient gas temperature and particle size on the ignition and combustion of aluminum particles at atmospheric pressure. Aluminum particles smaller than 100 μm were injected in hot product gases using flat flame burner with controlled temperature and composition. Qualitative results such as the ignition delay time and the burning time were obtained by using still photography.

Friedman and Macek observed that ignition occurred only when the ambient gas temperature ranges between 2210 and 2360 K. When ignition occurs, it is marked by a sudden increase in the luminosity of the particle. Friedman and Macek found that ignition was insensitive to the oxygen concentration. For example, the ignition limit, found to be 2270 K in stoichiometric gas composition, decreases

only by 60 K when 36% excess oxygen is present. On the other hand, the ignition delay time was found to be proportional to the square of the particles' diameter.

There are two modes of combustion, observed by Friedman and Macek, depending on whether fragmentation occurs or not. When fragmentation does not occur, hollow shells of oxide were observed to grow asymmetrically from the particle's surface, and the luminosity of the droplet was observed to be periodic. This indicates that the droplet was spinning while it is burning. By using excess of oxygen, the particles fragmented a few milliseconds after ignition occurs. Friedman and Macek found that an oxygen partial pressure of 0.38 atm was necessary for fragmentation to occur. The ambient gas temperature does not promote particle's fragmentation. However, fragmentation occurs as the ambient temperature reaches the boiling temperature of aluminum (2800 K).

In a second paper, Friedman and Macek [,7] studied the combustion of single aluminum particles with emphasis on the effect of water vapor on the ignition and combustion behaviors. Two different techniques were used to ignite the aluminum particles. In the first method, aluminum particles were injected in a stream of hot gases using flat flame burner. In the second technique, the aluminum particles were ignited in bomb vessel by means of combustion products of ammonium perchlorate flames with organic fuels added.

Friedman and Macek found that the necessary condition for ignition to occur is that the ambient gas temperature must reach

2300 K, the melting temperature of the aluminum oxide. The presence of water vapor does not effect much the ignition of aluminum; and the ignition delay time was found to be proportional to the square of the particles' diameter. This result was found to be the same as in the case of low moisture environment.

The combustion behavior of aluminum in a moisture-free environment depends on the oxygen concentration. When the oxygen mole fraction is less than 0.28, the burning of the aluminum droplet appears very sharp in the photographic film. In this regime, the combustion is characterized by the growth of oxide bubbles and the particle is burning only on one side as it is spinning at several thousand revolutions per second. The burning time was found to be approximately proportional to the 1.5 power of the particle diameter. In this regime, Friedman and Macek stipulated that aluminum boils right after ignition occurred. This causes the aluminum oxide to inflate asymmetrically; and the combustion reaction occurs at the bubble level where aluminum vapor fuel meets the oxygen. In the second regime where the oxygen concentration exceeds 38%, fragmentation was observed with particles' ejected in a random manner

The presence of water vapor does alter the combustion behavior of aluminum. The burning of aluminum in high moisture is slower than that in a low moisture environment. This can be explained by the fact that the reactant must diffuse through the condensed oxide layer. Friedman and Macek observed that in high

moisture the combustion is characterized by the growth of hollow shells of oxide adhered to the unburned part of the unconsumed metal. When combustion is complete, the combustion product consists of a hollow sphere having approximately the same size as the original particle. On the other hand the combustion of aluminum in low moisture is characterized by the continuous decrease of the original droplet.

Davis [1] discussed the importance of using aluminum powder as an addiditive in solid propellant systems. Theoretically, the addition of aluminum to the solid propellant fuel products increases the gas temperature because of the high flame temperature of the aluminum (3800 K). This substantial increase in the temperature will enhance the thrust efficiency of the solid propellants. In practice, however, this advantage is not accomplished; and it is found that sometimes the specific impulse falls below that of a nonmetalized solid propellants. Davis attributed this deficiency to two main reasons. First, the combustion of aluminum is not usually completed. This is due to the particles' aggregation, forming large agglomerates which slow down the burning rate of aluminum. The second problem consists of the fact that the aluminum oxide does not reach kinetic and thermal equilibrium during combustion. Therefore, Davis attempted to determine experimentally the optimum conditions that would enhance the thrust efficiency when aluminum is added. At atmospheric pressure, aluminum particles, ranging in size between 56 and 103 μm, were introduced in the center of a premixed flame of

controlled temperature and gas compositions. At higher pressure, the aluminum particles were ignited by burning ammonium perchlorate in a pressurized bomb with nitrogen.

Davis observed, using photographs, that the diameter of the flame zone is larger than that of the aluminum droplet. This detached flame, where the reaction zone is at a distance from the metal droplet, is similar to that observed when a hydrocarbon fuel burns. In addition, a trail of alumina(Al_2O_3) was observed in the wake region of droplet burning, indicating gas phase oxidation. The collected smoke of aluminum oxide was found to be hollow spheres. Davis also observed periodic luminosity of the aluminum droplet, which suggests that the droplet was spinning while it burned.

Davis found that the ignition delay time does not depend much on the oxygen concentration. On the other hand, the ambient gas temperature has a strong effect on the ignition delay time, which decreases as the ambient gas temperature increases. The strong dependence of the ignition delay time on the gas temperature can be related to the dominance of thermal heating in this regime. In contrast to the ignition delay time, the burning time strongly depends on the oxygen concentration but not much on the ambient gas temperature; and by keeping constant ambient gas temperature, the burning time is inversely proportional to the oxygen partial pressure.

At higher pressures, Davis noticed that the burning time decreases as the pressure increases. The burning time, however bec-

omes nearly constant as the pressure exceeds 6.8 MPa. The burning time was found to be proportional to the 1.8 power of the particle's diameter at high pressures (>6.8 MPa). Davis observed that at these high pressures, the aluminum droplet burns like a hydrocarbon fuel droplet; and the effect of the oxide condensation is diminished. Based on his study Davis recommended that in order to take advantage of the high flame temperature of aluminum, the aluminum particles should be as small as possible; and the operating pressure should be above 6.8 MPa.

Brzustowski and Glassman [8] developed a theoretical model for the combustion of aluminum and magnesium. Brzustowski and Glassman argued that aluminum can burn only in the vapor phase because the boiling temperature of aluminum oxide (3800 K) exceeds the boiling temperature of aluminum metal (2750 K). Glassman and Brzustowski extended a developed model of hydrocarbon fuel droplet combustion by taking in account the burning characteristics of aluminum droplet. These characteristics includes: 1) flame temperature fixed at the boiling temperature of aluminum oxide, 2) effect of the condensed oxide on the oxygen diffusion and 3) evaporation of the metal is not as fast as the diffusion processes occurring in the gas phase.

The model can be briefly described as a spherical aluminum droplet surrounded by a concentric flame zone. The shell between the droplet and the flame is a stagnant film through which the vapor and oxidizer were diffused stochiometrically in the reaction zone. To

avoid mathematical complications, the pressure gradient and the diffusion of aluminum oxide into the droplet surface are not considered. Glassman and Brzustowski derived the energy equation by applying the conduction and enthalpy equations at the boundary. Furthermore, the diffusion and evaporation equations were derived using Fick's law and Knudsen-Languimuir equation, respectively for a binary system. Since these equations have to be solved numerically for each set of input, the gross trend of the burning characteristics (burning rate, flame structure) can not be obtained. Therefore, Brzustowski and Glassman developed a simplified model which reveals the general behavior of the burning characteristics of aluminum droplet. In the simplified model, the evaporation equation is ignored by assuming that the evaporation rate is sufficient to keep up with the diffusion processes occurring in the reaction zone.

Results from the simplified model are presented in Figures 2.1 and 2.2. In these figures the dimensionless fuel flux, the ratio of the flame radius to the droplet radius r_B/r_A and the dimensionless burning rate were respectively plotted as a function of the dimensionless oxidizer flux, the radiant heat transfer parameter σ_{AB} and the transfer number. The radiation parameter is varied using different particles' diameter and also by varying the ambient pressure range between 0.1 and 5 MPa. The transfer number B is basically a factor dependant on the latent heat of the metal. As can be seen from Figure 2.1, r_B/r_A decreases with an increase of the oxygen flux. This result indicates that by increasing the oxygen flux

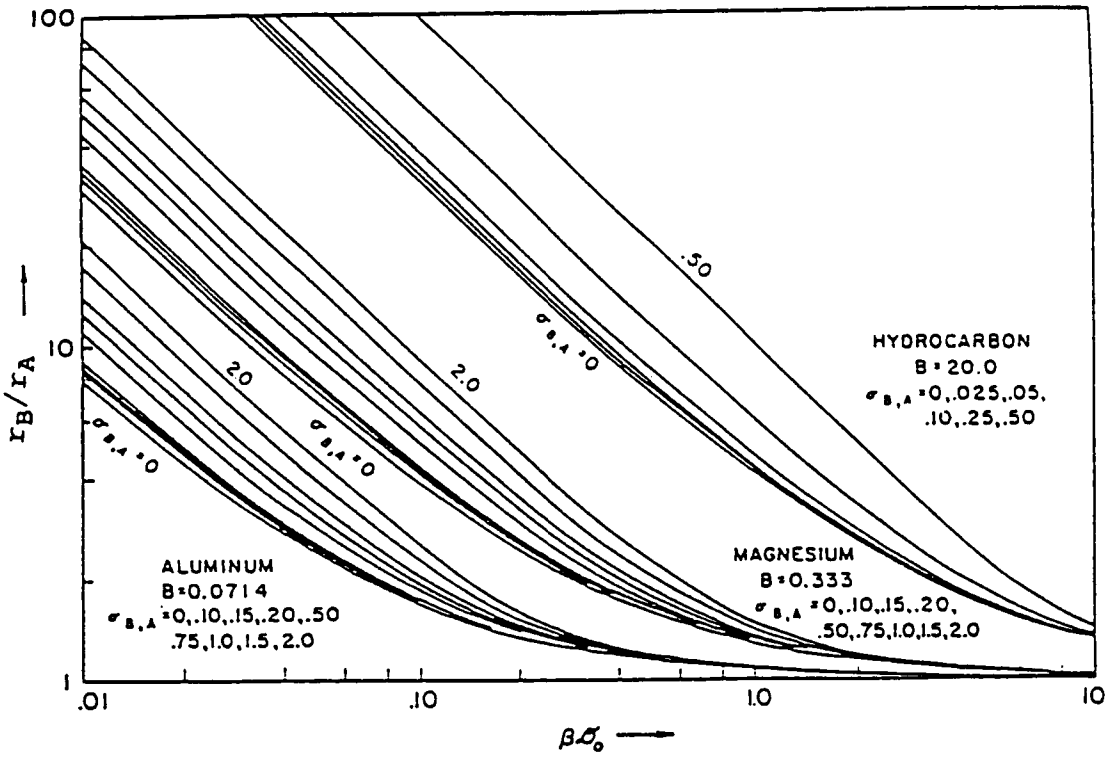

FIGURE 2.1 Ratio of the Flame Radius r_B to the Droplet Radius r_A as a Function of the Dimensionless Oxidizer Flux βD_O, the Transfer Number B, and the Radiation Parameter $\sigma_{B,A}$ [8].

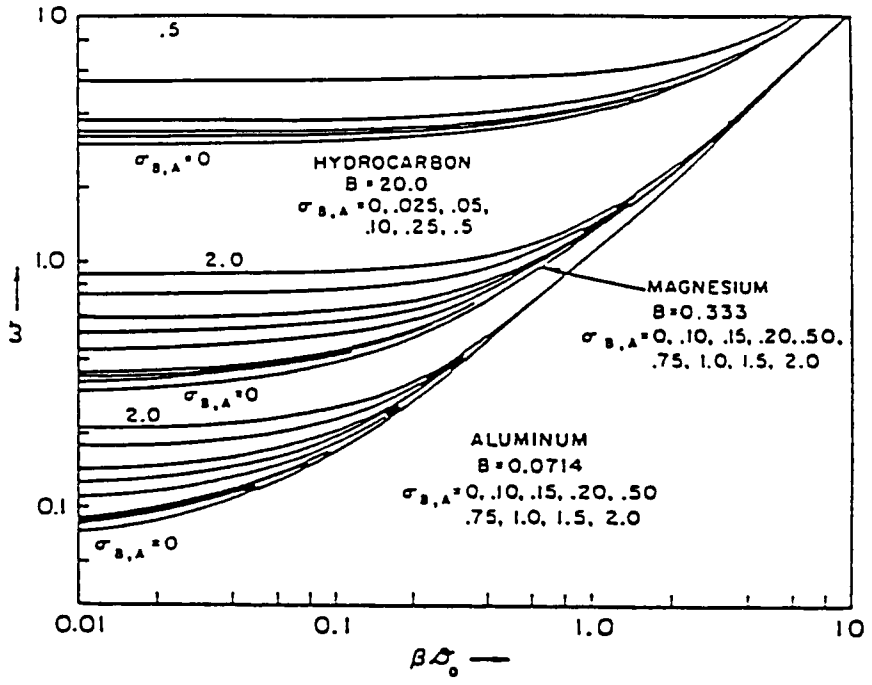

FIGURE 2.2 Dimensionless Burning Rate ω as a Function of the Dimensionless Oxidizer Flux βD_O, the Transfer Number B , and the Radiation Parameter $\sigma_{B,A}$ [8].

more fuel is needed to maintain the stoichiometry of the reaction. On the other hand, the flame radius increases by increasing the transfer number. This result can be explained by recognizing the dependency of the transfer number on the latent heat of the metal. Therefore, the higher the latent heat is, the greater the temperature gradient will be at the surface causing a larger film in the reaction zone. The increase of radiant heat transfer parameter increases r_B/r_A. Figure 2.2 shows the effect of the oxidizer on the burning rate. At lower oxidizer flux (βD_O), the burning rate increases proportionally with the oxidizer flux. On the other hand, at very high oxidizer flux (βD_O) values the burning rate increases slowly. This can be related to the fact that the flame stand-off ratio does not change much at very high oxidizer flux (see Figure 2.1).

Even though the Glassman's model provides important features about the burning characteristics of aluminum droplets, this model has some limitations. First, this model deals with the burning of a single aluminum particle in an isolated environment, ignoring the particle's interaction with other burning particles. Second, the steady state assumption is poor because repeatedly the experimental observations show that the combustion of aluminum is characterized by unsteady effects such as fragmentation, spinning and jetting of the droplet. Third, the aluminum droplet does not burn symmetrically; and it has been shown that in some environments aluminum burns only on one side. Finally, the accumulation of the oxide on the droplet

is not considered in this model.

Bartlett et al., [9] proposed a different model from that developed by Glassman and Brzustowski. Bartlett et al., argued that the stability of the condensed oxide phase and the high boiling temperature of aluminum metal, suggest that the controlling process in the aluminum combustion consists of the transport of aluminum vapor through the oxide layer, surrounding the aluminum droplet. This mode of combustion is strongly backed by the combustion products which were found to be hollow spheres. In conjunction with the theoretical model, Bartlett et al., also performed experiments on the combustion of aluminum particles. These particles, ranging in size between 10 and 50 μm, were ignited in an oxygen-methane flame and observed using a high-speed camera and rotating light chopper.

Bartlett et al., observed that ignition occurs only when the metal oxide reaches its melting temperature (2300 K). The ignition is purely dominated by gas heat conduction through the oxide layer. In addition, Bartlett et al., observed fragmentation and a spiral motion of some burning droplets. The combustion products were collected and morphology analysis was carried out. The combustion products were generally spherical particles ranging in size from less than 1 μm to a greater size than the original ones. The combustion products also included hollow oxide spheres containing some unburned metals. Therefore, Bartlett et al., suggested that any combustion modeling of aluminum should take into account the morphology of the combustion product; especially, the hollow oxide spheres.

The combustion model suggested by Bartlett et al., is based on the assumption that the diffusion of the metal vapor through the oxide layer, surrounding the molten droplet is the rate controlling step in the combustion of aluminum particle. In this model, the combustion of aluminum comprises of two different modes as shown in Figure 2.3 :1) combustion without metal evaporation and 2) combustion with metal evaporation. In the first mode, the combustion of aluminum occurs in the temperature range between the ignition temperature (2300 K) and the boiling temperature of aluminum metal (2750 K). In this mode the oxide layer is an obstacle for the metal evaporation provided that the vapor pressure is less than the system pressure. The major heat source is generated by chemical reactions at the oxide layer. In the second mode where the boiling point of aluminum is reached, the metal begins to evaporate, forming a vapor film between the oxide layer and the molten droplet. The fuel vapor then diffuses through the oxide layer. Consequently, the reaction occurs at the oxide layer instead in the gas environment as suggested by Glassman and Brzustowski. The oxide shell radius decreases or increases depending on the mass evaporation rate of the metal which must be equal to the rate of oxidation of metal at the oxide. Bartlett et al., explained fragmentation and spinning of the particle by the excessive expansion of the oxide layer in which rupture occurs and some small droplet is ejected.

Prentice [10] studied the combustion of pulsed-heated single aluminum particles using two different techniques: Xenon flash heat-

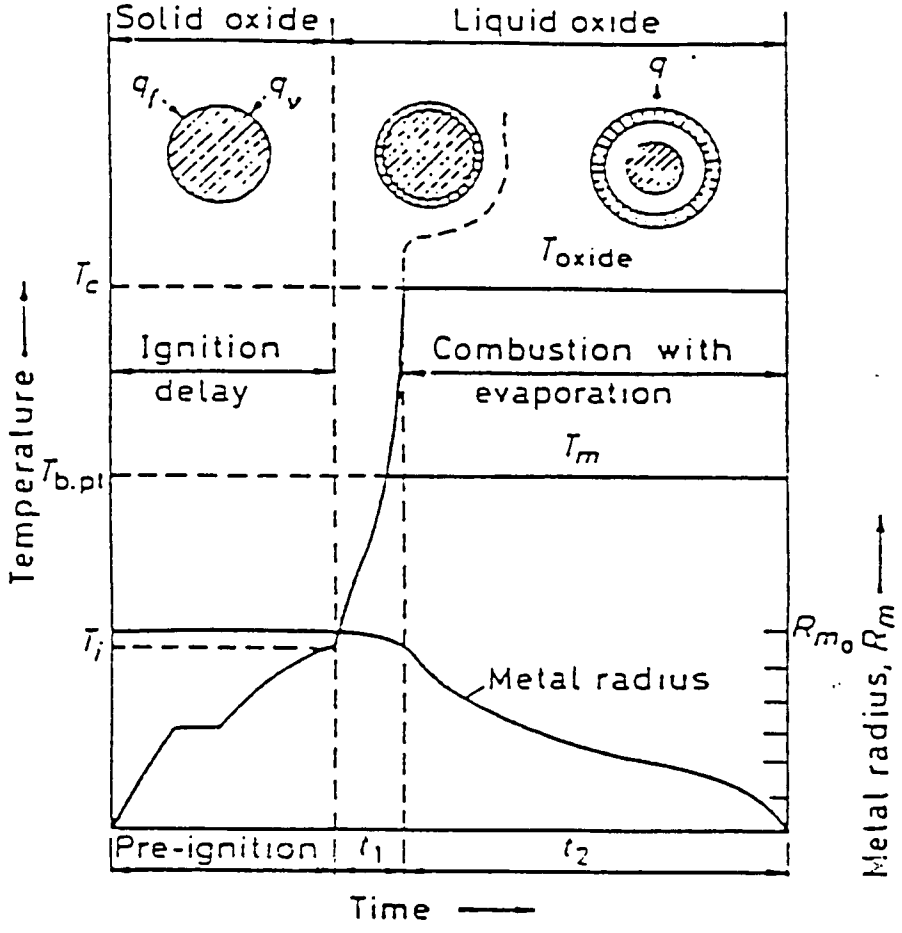

FIGURE 2.3 Schematic Plot of Metal Oxide Temperatures and Metal Droplet Radius During the Pre-Ignition and the Two Combustion Periods [9].

ing and Nd-glass laser pulse. The ignition of aluminum particles using xenon flash heating is conducted by dropping an aluminum particle in a narrow glass pipe, surrounded by a helical xenon flash tube. As the particle reaches the enclosed lamp, the latter explodes giving a high intensity thermal pulse which ignites the particle. In the second technique, the aluminum particle was ignited by a laser pulse. The aluminum particles are actually square foils cut to give droplets ranging in size between 100 and 500 μm. The experiment were mainly performed in air and oxygen/argon (20/80) environments.

Prentice observed two different modes of combustion depending on whether or not the oxide product accumulates on the droplet surface. If the oxide accumulates on the surface, spinning, jetting and fragmentation have been observed during the later burning stages of aluminum droplets. On the other hand, the absence of oxide accumulation results in complete consumption of the particle with no spinning, no jetting and no fragmentation.

In the O_2/Ar environment, the aluminum droplet burns in a straight forward manner without oxide accumulation; and the combustion behavior of the aluminum droplet resembles the vapor diffusion model suggested by Glassman and Brzustowski, which will be discussed later. The burning time, measured photometrically, was found to be linearly proportional to the particle diameter. In an air environment, Prentice observed an accumulation of the oxide products on the droplet surface, which led to a more complex burning behavior consisting of jetting, spinning and fragmentation. The

morphology study of a quenched aluminum droplet has shown that the oxide correspond to a "fumarole" shape rather than to a lens cap, observed in a previous quenching study utilizing a lower power optical microscope. Furthermore, the oxide surface exhibits some smoke patterns, which suggest that the fuel vapor is diffusing outwardly through the oxide globule.

Prentice also investigated the effect of pressure on the particle fragmentation in dry air. He found out that the particle fragments weakly in air and as the pressure is increased to 0.24 MPa, the fragmentation becomes sporadic, and ceases at a pressure of 0.4 MPa. In addition, the particle fragmentation was found to be inversely proportional to the applied pressure. In another experiment, Prentice noticed that the introduction of a small amount of nitrogen (5%) in an oxygen/argon (20/80) environment caused the particle to spin; and as the amount of nitrogen was increased to 10%, he observed spinning and sporadic fragmentation at later stages of the aluminum droplet burning. Based on these observations, he concluded that nitrogen plays a major role in adhering the oxide to the droplet surface and it is this that results in jetting, spinning and fragmentation of the particle. Furthermore, carbon monoxide was found to promote oxide accumulation on the droplet surface.

Wilson and Williams [11] experimentally studied the combustion of single aluminum particles. In their experiments, they tried to provide an idealized environment that conforms with the assumptions normally made in the modeling of aluminum combustion. These

assumptions include: burning symmetry of the droplet, steady state burning, negligible convection and radiation. In addition, they hoped to verify the "d^2" law; i.e., diffusion-controlled, through this technique. Thus, the aluminum particles were chosen as small as possible (50-90 μm). Argon was used as a dilution gas to suppress and minimize the oxide accumulation (known to create complex phenomenon such as fragmentation, jetting and spinning). The aluminum particles were ignited using laser pulses, and the burning history was observed using cinematomicrography.

Wilson and Williams observed a detached flame, surrounding the burning droplet. This flame is similar to that associated with the burning of a hydrocarbon fuel droplet. The "d^2" law (corresponding to the vapor diffusion model) was not definitive and the burning rate exponent "n" was found between 1 and 2. However, Wilson and Williams noticed, through data reduction, that there was a consistency favoring n=2. Furthermore, the flame stand-off ratio was found to be inversely proportional to the oxygen mole fraction. The effect of pressure could not be determined because of the small pressure range (0.1-0.5 MPa) in which the experiments were carried out.

Wilson and Williams observed that ignition does not occur for oxygen partial pressure below 0.02 MPa, and as the partial pressure exceeds 0.1 MPa, the droplet moves out of view. In addition, they investigated the effect of laser flux output on the burning mechanism of the aluminum droplet. They found that there is a threshold energy below which the ignition is delayed and the oxide product

accumulates on the surface. Above this threshold, the flame structure is symmetrical and it resembles to the flame zone of a hydrocarbon fuel droplet.

Law [12] developed a theoretical model for the vapor-phase combustion of metal particles. In contrast to Glassman's model, this model takes into account the accumulation of oxide on the droplet surface and motion of the vapor oxide. In this model , Law developed four different combustion models, depending on the experimental observations and the environmental conditions. These models are:1) combustion with oxide accumulation on the surface (model A), 2) combustion without oxide accumulation on the surface (model B), 3) combustion in dilute environment (model C) which obtained by lowering the flame temperature and 4) combustion in enriched environment (model D), obtained by increasing the flame temperature.

In his model, Law used some combustion features which characterize the burning of a hydrocarbon fuel droplet. These features include: steady state burning, spherical symmetry of the flame and isobaric environment. Law further assumed that the vapor fuel and the oxidizer fuel diffuse instantaneously into the reaction zone which is detached from the droplet surface. The flame temperature is fixed by the boiling temperature of aluminum oxide (3800 K) in order to satisfy the Glassman's criteria for vapor phase combustion However, in the dilute (cool) environment, the flame temperature is assumed to decrease so that less heat would be lost to the environ-

ment. During combustion, a fraction of the oxide diffuses inwardly into the droplet surface and condenses instantaneously, whereas the remaining diffuses outwardly and condenses in the atmosphere. The motion of the vapor oxide, as described by Law, depends on the motion of the bulk gases velocities of the inward (V_1) and outward zones (V_2). Therefore, there are four possible motions of the oxide products: (i) for $V_1>0$ and $V_2>0$, the vapor oxide products are convected outside; (ii) for $V_1>0$ and $V_2<0$, the vapor products will be trapped at the flame; (iii) for $V_1<0$ and $V_2<0$, the vapor oxide will diffuse inwardly and condenses on the droplet surface; (iv) For $V_1<0$ and $V_2>0$, this condition can not exist. In mode (ii), the trapped oxide does not effect the burning mechanism because the combustion products is dispersed over a large area in the flame.

Results from the theoretical model are shown in Figures 2.4 and 2.5. Figure 2.4 represents the nondimensionalized mass burning rate and the nondimensionalized flame stand-off ratio as a function of the oxygen mole fraction (Y_O) for model A, C and D. The mass burning rate is found to increases almost linearly with the Y_O. The ambient temperature T does not affect much the burning rate. For the flame stand-off ratio, there are two regimes depending on the ambient temperature. For $T_{ambient} < T_{droplet\ surface}$, the stand-off ratio rapidly increases with increasing of oxygen mole fraction Y_O. On the other hand, the stand-off ratio rapidly decreases with increasing oxygen mole fraction Y_O when $T_{ambient} > T_{droplet\ surface}$. Furthermore, Figures 2.4a and 2.5a provide an opportunity to see the effect of the

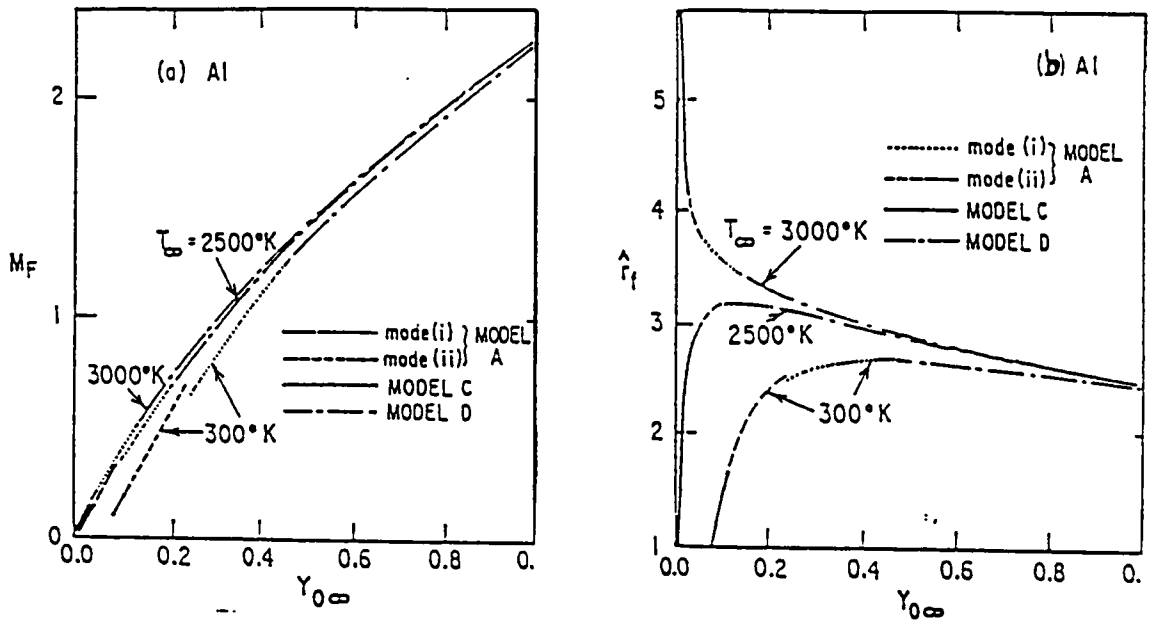

FIGURE 2.4 (a) Nondimensionlized Mass Burning Rate M_F and (b) Nondimensionlized Flame Stand-off Ratio as Functions of Y_O in Various Ambient Temperatures for Aluminum Burning [12].

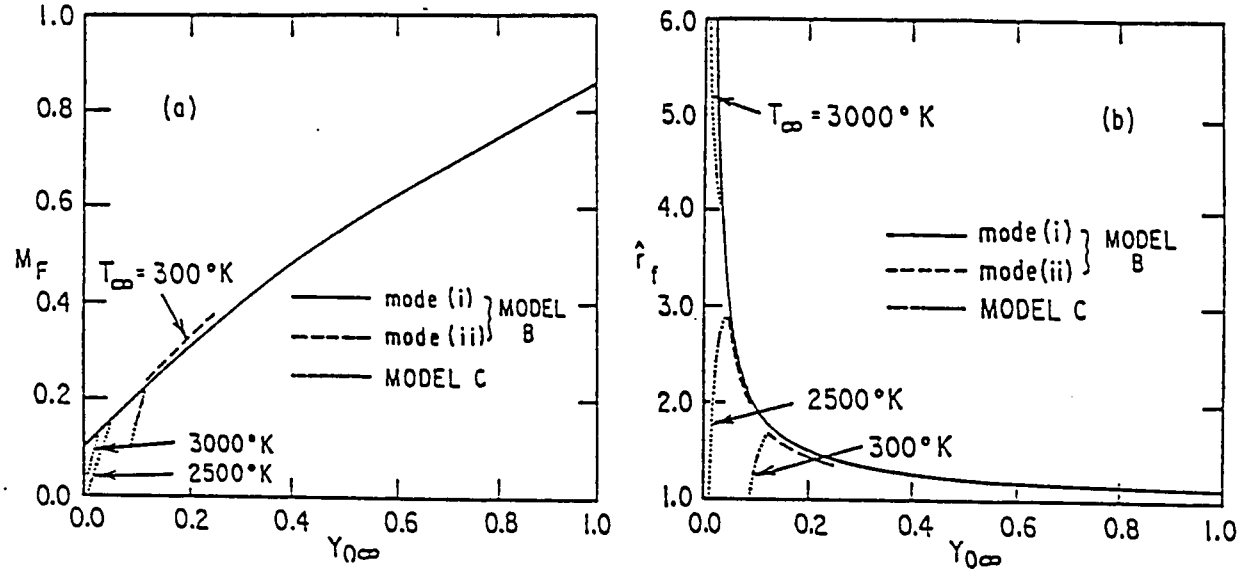

FIGURE 2.5 (a) Nondimensionlized Mass Burning Rate M_F and (b) Nondimensionlized Flame Stand-off Ratio as Functions of Y_O in Various Ambient Temperatures for Aluminum Burning Without Surface Condensation [12].

oxide accumulation on the surface on the burning rate of aluminum droplet. As can be seen from these two figures, the accumulation of the oxide on the droplet surface enhanced the mass burning rate. For example the mass burning rate has been reduced by a factor of 1.7 at $Y_O = 0.2$ when the oxide accumulation on the droplet surface is suppressed.

2.2 IGNITION AND COMBUSTION OF ALUMINUM AGGLOMERATES .

A literature survey on the ignition and combustion of aluminum agglomerate, has produced only two papers in which all experiments were performed at atmospheric pressure.

In the first paper, Wong and Turns [13] studied the ignition characteristics of aluminum/JP-10 slurry fuel droplets. These slurry droplets, ranging in size between 300 and 800 μm, were exposed to the hot product gases of a flat flame burner; and the ignition history was observed using high speed cinematography. The effects of oxygen concentration, ambient gas temperature and initial droplet diameter on the ignition of the aluminum slurry fuel droplets were investigated.

From high-speed cinematography, Wong and Turns observed that slurry droplets ignite in two distinct stages. As the droplet is exposed to the hot gases, the liquid fuel carrier evaporates and burns leaving behind a porous agglomerate. The aluminum agglomerate then heats up with a protective oxide layer, formed on the agglomer-

ate surface. During this time the agglomerate's integrity is maintained. As the agglomerate temperature increases, the aluminum particles melt and coalesce into a single molten droplet which can no longer be held by the oxide layer. At this point, a diffusion flame surrounding the droplet is observed. Wong and Turns defined the ignition delay time as the time elapsed between the exposure of the slurry droplet to the hot gases and the appearance of the flame around the droplet.

Wong and Turns found out that the ambient gas temperature has a strong influence on the ignition delay time which decreases as the ambient gas temperature increases as shown in Figure 2.6b. But no ignition, however occurs below 1300-1450 K. On the other hand, the ignition delay time does not depend much on the oxygen mole concentration; i.e., high oxygen mole fractions result in a small decrease in the ignition delay times (see Figure 2.6a). This can be explained by the fact that the thermal effect has a stronger influence in the pre-ignition regime than does the chemical effect. The ignition delay time is also increased by increasing the initial droplet diameter as shown in Figure 2.7. The ignition delay time of aluminum slurry agglomerates,obtained in the study is between 0.2 and 1.2 s.

Wong and Turns developed a theoretical model for the ignition of aluminum slurry droplets. This model is essentially based on the experiments in which Wong and Turns observed that the preignition histories of aluminum slurry droplets are composed of two different stages: 1) evaporation and combustion of the JP-10 liquid fuel and 2)

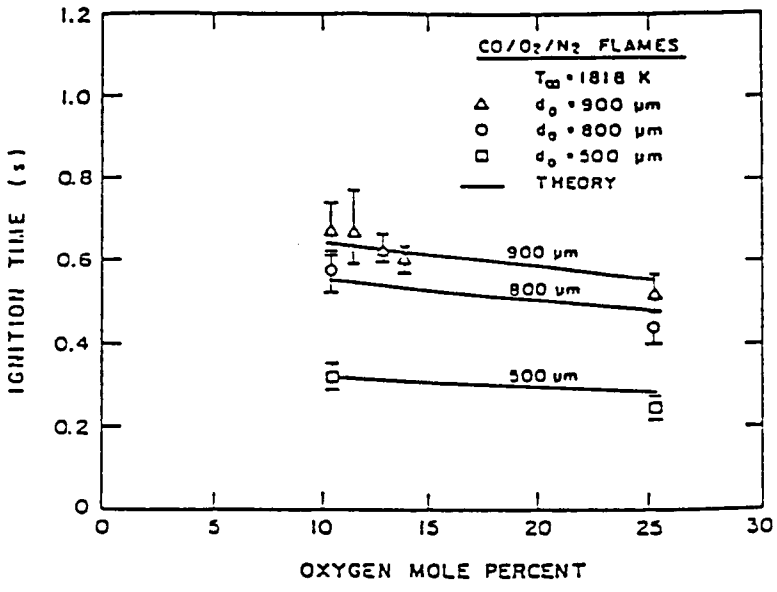

(a)

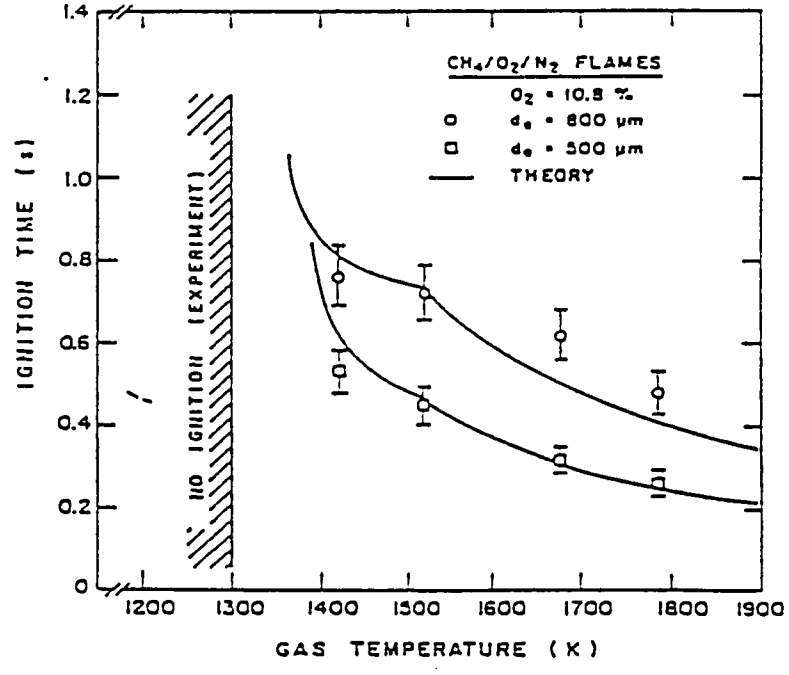

(b)

FIGURE 2.6 Ignition Times Versus (a) Oxygen Mole Fraction and (b) Gas Temperature for Al/JP-10 Slurries [13].

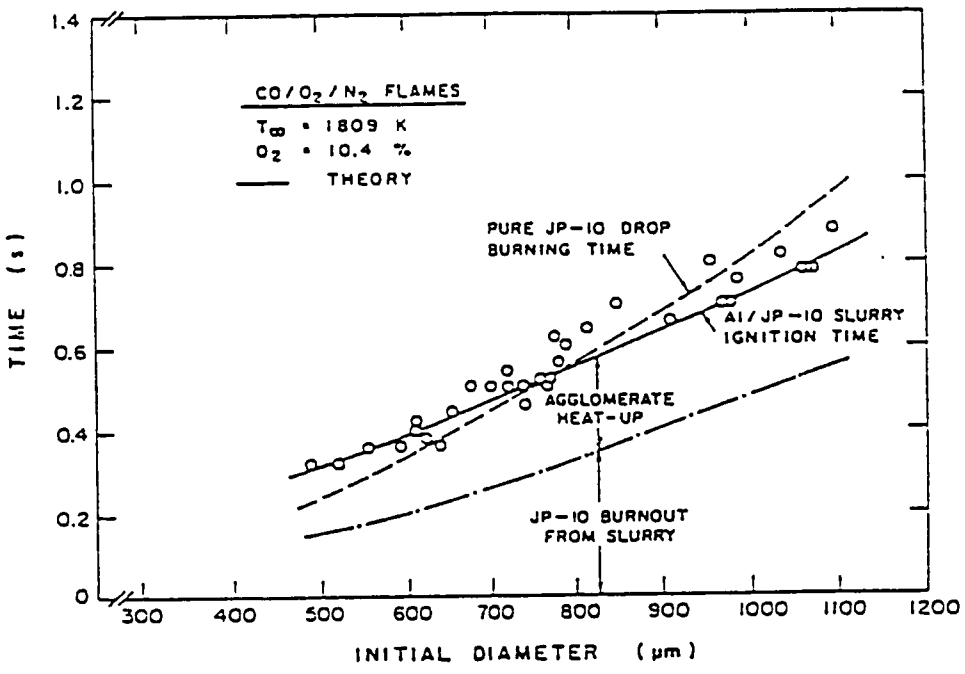

FIGURE 2.7 Ignition Times Versus Initial Droplet Diameter for Al/JP-10 Slurries [13].

heating of the dry aluminum agglomerate up to its oxide melting point (2300 K). Therefore, gas and liquid phase equations were derived, using mass and continuity equations, to account for the fuel combustion rate during the first stage of the pre-ignition regime. In the second stage, the rate of change the agglomerate's temperature is determined. In this stage, the change of the temperature rate depends on convection, radiation and chemical reaction. The results of this theoretical model were compared with experimental data in Figures 2.6 and 2.7. The theoretical results correlate with the experimental data.

In a second paper, Turns and Wong [14] studied the combustion phenomena of aluminum agglomerates after the liquid fuel carrier burned out. They investigated the combustion behavior of the agglomerates by varying the following parameters: initial droplet diameter, oxygen mole fraction, gas flame temperature and water vapor content.

Turns and Wong observed that after the liquid fuel is burned out, the agglomerate becomes porous and it has a fuzzy image. As the temperature increases, the agglomerate heats up and coalesces into a molten droplet of aluminum. This coalescence is marked by the sharp decrease in the agglomerate's diameter. Because of the high melting temperature of the aluminum oxide layer formed around the droplet, the ignition is delayed until the droplet's inner temperature reaches 2300 K; i.e., the melting temperature of aluminum oxide. The ignition of aluminum is characterized by the appearance of a detached

diffusion flame. During combustion, some of the oxide vapor is convected out and the remainder is diffused inward to condense on the droplet surface. Even though the vapor phase transport dominates the combustion process of aluminum agglomerates, the accumulation of the oxide vapor makes it a complex process. In their study, the total burning time is defined as the time elapsed between the coalescence of the droplet and the instance at which no more oxide vapor is observed.

By varying the initial diameter,oxygen mole fraction,gas flame temperature and the water vapor content, Turns and Wong found out that the oxygen mole fraction has a strong effect on the total burning time which increases as the oxygen concentration decreases (see Figure 2.8). On the other hand, an increase in the ambient gas temperature only slightly decreases the burning time as can be seen in Figure 2.9a. By increasing the initial diameter, the total burning time also increases (see Figure 2.9b). In addition, violent eruptions along with partial fragmentation and jetting were observed in a wet environment but not in a dry environment. The diffusion flame in the wet environment is closer to the droplet than that in the dry one. Furthermore, in a wet environment, the droplet is encapsulated by the oxide layer causing the burning time to be shorter than that in a dry environment.

In an attempt to understand the combustion behavior of aluminum-based slurry agglomerates, Turns and Wong developed a model for the combustion of aluminum agglomerate. This model, as

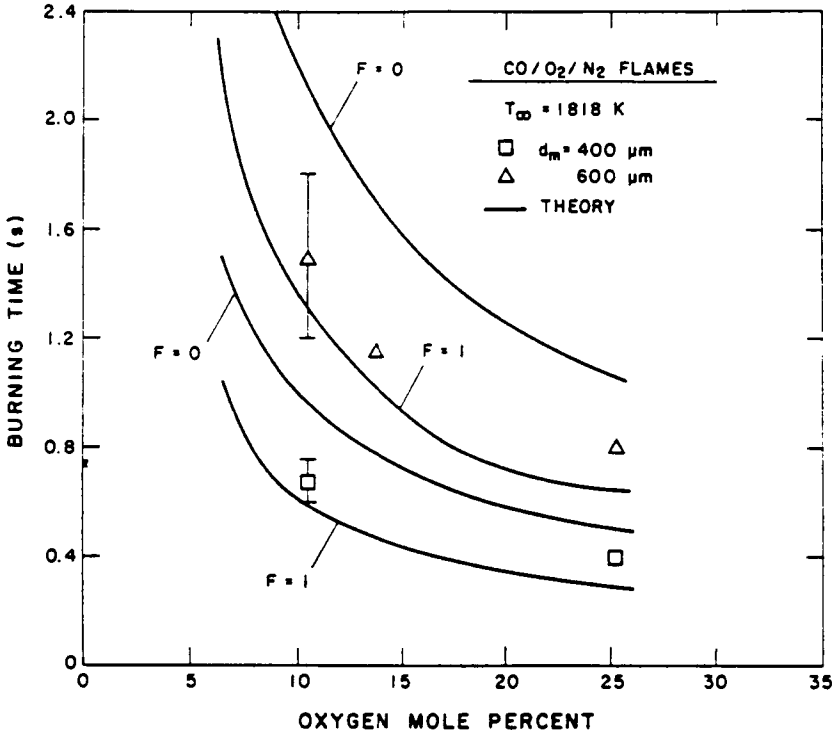

FIGURE 2.8 Aluminum Droplet Burning Times Versus Oxygen Mole Fraction [14].

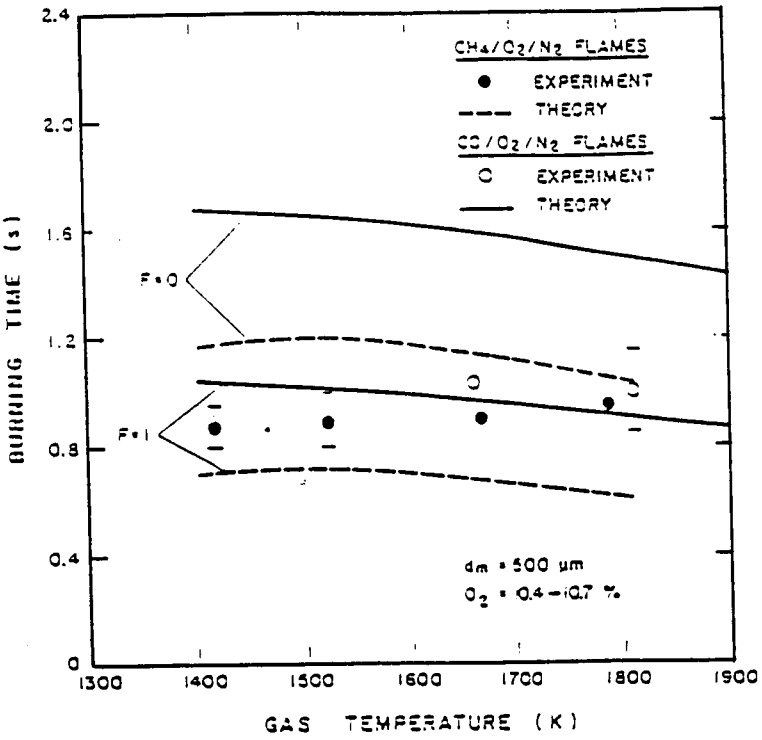

(a)

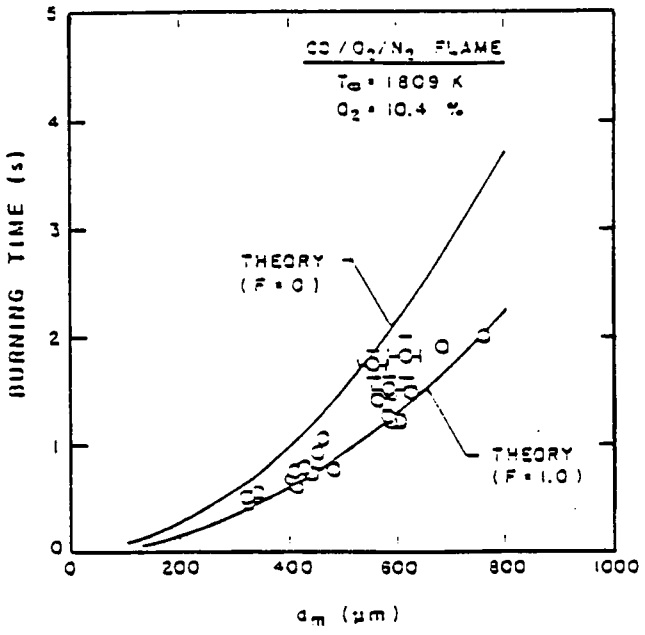

(b)

FIGURE 2.9 Aluminum Droplet Burning Times Versus (a) Ambient Gas Temperature for Wet and Dry Environments, and (b) Diameter for Coalesced Aluminum Slurry Agglomerates[14].

seen in Figure 2.10, is basically an extended work of the model developed by Law. In this model, the vapor fuel and the oxidizer are assumed to react stoichiometrically in the reaction zone. The oxide boiling temperature of the oxide (3800 K) and the boiling temperature of aluminum (2800 K) are respectively taken to be the flame temperature and the droplet surface temperature. In order to maintain the flame temperature at the oxide boiling temperature, the oxide is assumed to be vaporized. This vapor oxide is partly convected out in the wake region and the other part is diffusing back into the droplet surface forming a spherical segment (see Figure 2.10).

A general trend of the combustion history of aluminum agglomerates is illustrated in Figure 2.11. This figure shows continuous depletion of the aluminum mass is accompanied by the continuous accumulation of aluminum oxide on the droplet surface. The theoretical results are plotted in Figures 2.8 and 2.9; and as one can see, there are two theoretical curves in each figure for F=0 and F=1. These two curves represent the cases when the accumulated oxide is impermeable (F=1) and when the oxide has sufficient cracks so that aluminum vapor can diffuse through the oxide layer (F=0). The experimental data can be seen to fall between these two curves.

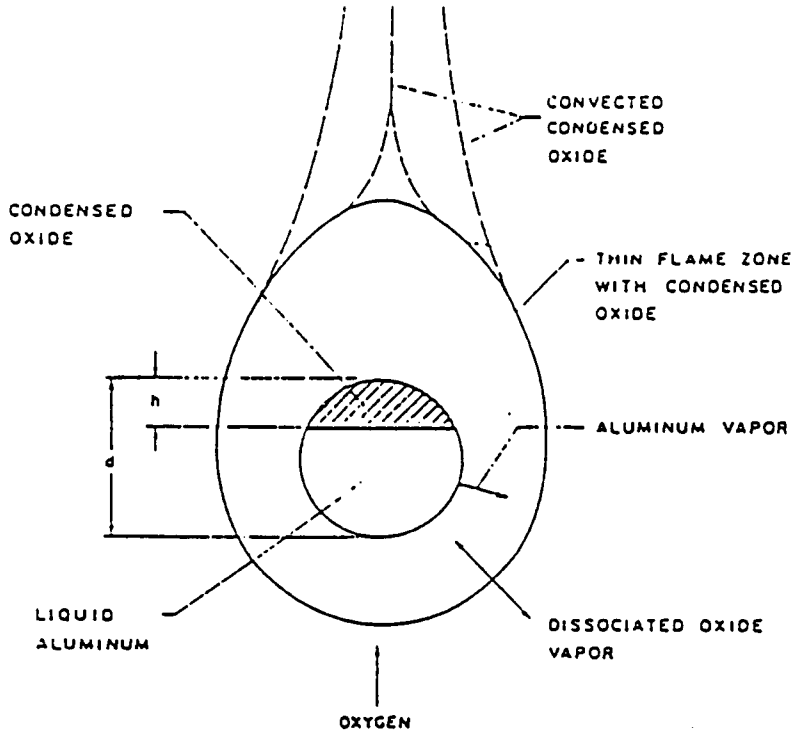

FIGURE 2.10 Aluminum Combustion Model Incorporating Oxide Accumulation [14].

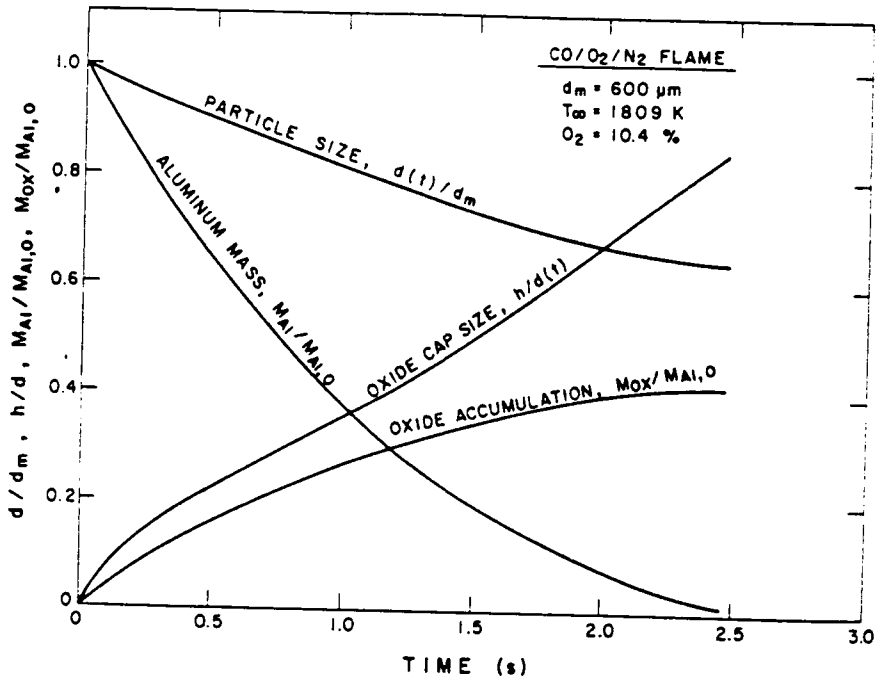

FIGURE 2.11 Predicted Life History of Aluminum Agglomerate After Ignition [14].

CHAPTER 3
EXPERIMENTAL APPARATUS AND PROCEDURE

This chapter will briefly discuss the experimental apparatus and procedure used in the present investigation. An overview of the experimental method is outlined in section 3.1. Section 3.2 presents the test conditions. The aluminum agglomerate production technique is addressed in section 3.3. A brief discussion of experimental apparatus is outlined in section 3.4. Sections 3.5 and 3.6 present the experimental procedure and methods of data analysis, respectively.

3.1 OVERVIEW OF EXPERIMENTAL METHOD

In this study the effect of the ambient pressure on the ignition and combustion of aluminum agglomerates was investigated in quiescent O_2/N_2 (20/80) atmospheres.

The probe-supported aluminum agglomerate was mounted vertically in a high pressure combustion chamber. The combustion chamber is mounted on a stand which can be displaced vertically and horizontally in order to adjust the position of the agglomerate toward the laser beam. Ignition of the aluminum agglomerate is achieved by using a focused CO_2 laser pulse. As seen from the overall schematic of the experimental apparatus in Figure 3.1, the laser beam irradiates the front and back surfaces of the agglomerate simultaneously. This

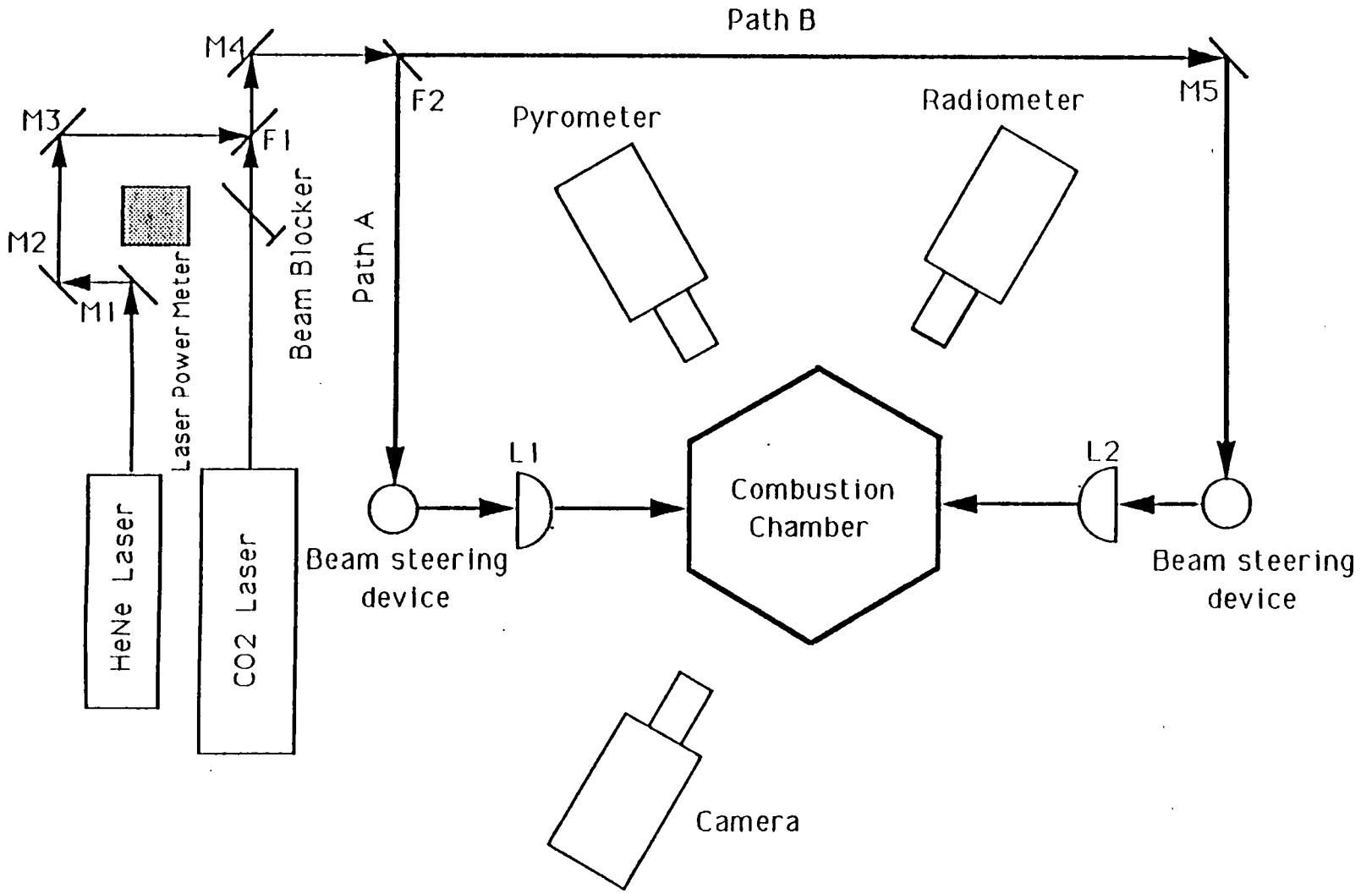

FIGURE 3.1 Schematic Layout of the Experimental Setup

is accomplished by splitting the CO_2 laser beam using a series of mirrors(M), ZnSe beam splitter(F1), Ge beam splitter(F2) and lenses (L1) and (L2). By irradiating both sides of the agglomerate, localized heating of the aluminum agglomerate can be prevented.

The alignment of the CO_2 laser beam with the agglomerate is achieved by using a He-Ne laser. The He-Ne laser is introduced to the path of the CO_2 laser path by using a ZnSe beam splitter(F1). Once alignment has been achieved, the CO_2 laser beam is introduced into the system by using a solenoid-activated beam blocker. This beam blocker is also connected to a timer circuit. By energizing the solenoid, a spring loaded arm swings out of the way of the beam, creating a shutter. The duration of the laser pulse can be varied from 40 ms to 1 s. The timer circuit is used to activate the data acquisition system,the radiometer and the two-color pyrometer.

Prior to performing the experiment, the CO_2 laser power was measured by directing the beam toward the power meter. This is accomplished by mounting a mirror on the beam blocker. The laser power can be varied either by varying the CO_2 flow rate or the current of the power supply.

A two-color pyrometer was used to measure the surface temperature of aluminum agglomerate. The two-color pyrometer operates in the near-infrared at two narrow spectral regions centered at 0.8 and 1.0 μm. In conjunction with the two-color pyrometer, a broad band radiometer was employed to determine the total burning time of the agglomerate. The radiometer operates in a

broad spectral region from 0.3 to 1.1 μm. To study the phenomenological events of the combustion aluminum agglomerate, a high-speed camera, capable of 4000 frames per second, was used.

3.2 TEST CONDITIONS

In the present study, all the tests were performed in a quiescent atmosphere of oxygen/nitrogen (20/80) environment. The pressure was varied from 0.1 to 4.3 MPa. Prior to each test, the gas mixture was desiccated before induction in the combustion chamber in order to avoid water vapor effects on the combustion behavior of the aluminum agglomerate. A laser power of 31 W was used throughout the tests. The laser pulse duration, required for ignition, ranged between 80 and 100 ms.

3.3 ALUMINUM AGGLOMERATES PRODUCTION TECHNIQUE

Aluminum agglomerates were produced at the tips of SiC fibers using a technique developed in this laboratory. Aluminum powder of 99% purity and 3 μm in size was mixed with alcohol and deposited at the end of a silicon carbide (SiC) fiber of 150 μm in diameter using a hypodermic syringe. The alcohol evaporated rapidly leaving behind a thin coating of solid aluminum powder. Additional application of the droplet resulted in a nearly spherical aluminum agglomerate at the end of the fiber. A comparator microscope was used to both measure

the agglomerate diameter and to assure the uniformity of the agglomerates' shape. These agglomerates were given at least one week to dry. A typical aluminum agglomerate is shown in Figure 3.2.

3.4 BRIEF DESCRIPTION OF EXPERIMENTAL APPARATUS

This section briefly described the experimental apparatus used in this study. A detailed description of the experimental apparatus can be found elsewhere [15].

3.4.1 HIGH PRESSURE COMBUSTION CHAMBER

The combustion chamber, shown in Figure 3.3, includes of the enclosure flange and the main body. The enclosure flange has a diameter of 12 cm, a thickness of 100 mm; and is machined of 316 stainless steel. The enclosure flange is secured to the main body by 8 machine screws. To prevent gas leakage, an O-ring seal is utilized for sealing between the flange and the main body. The main body, hexagonal in shape, is also machined out of 316 stainless steel. It has an internal diameter of 6.5 cm and a wall thickness of 3.5 cm. The main body is designed such that the internal volume (0.8 l) will be adequate to prevent pressurization due to excessive heating from the burning droplet.

There are six windows on the periphery of the main body. These windows are equally spaced and placed at angle of 90° with

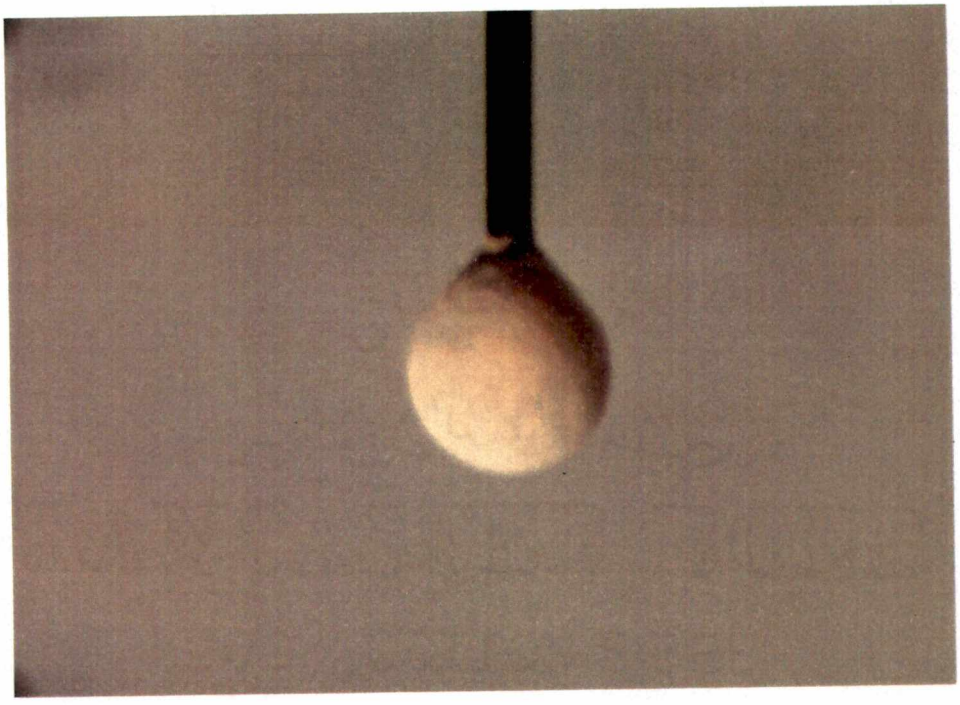

FIGURE 3.2 Photomicrograph of a Typical Aluminum Agglomerate

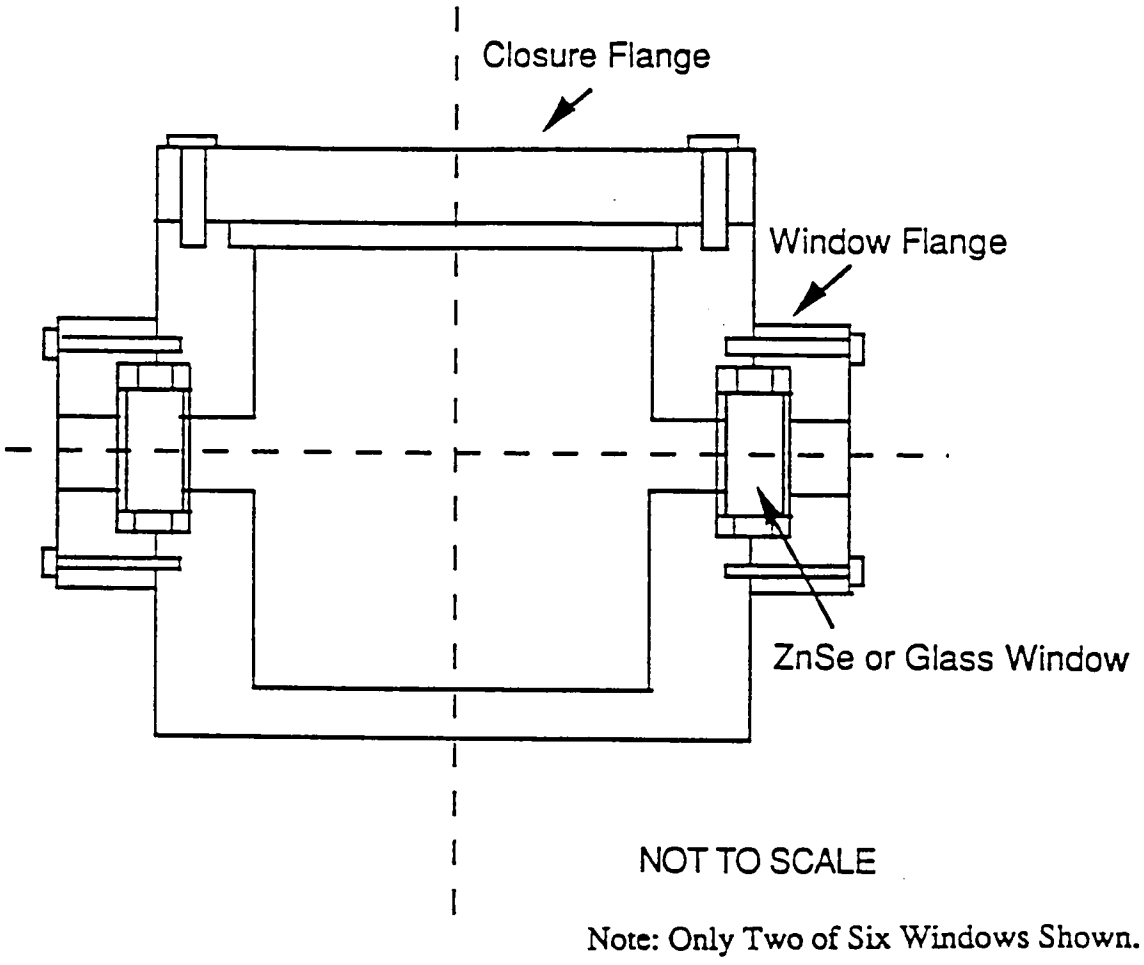

FIGURE 3.3 Cross-Sectional View of the Combustion Chamber.

respect to the axis of the combustion chamber. Two of these windows, which are made of ZnSe, are used to transmit the 10.6 μm laser beam. Three of the remaining four windows provide optical access for the pyrometer, radiometer and the high-speed camera. The remaining window is used for observation during the course of the experiment.

3.4.2 CO2 LASER SYSTEM

A detailed discussion of the CO_2 laser can be found elsewhere [15], only a brief discussion is given here. Figure 3.4 shows the general structure of the CO_2 laser system. The laser optical resonator is composed of a gold coated spherical concave copper mirror (100% reflector) of 10 m radius of curvature and ZnSe flat partial reflector (35% reflection). The two mirrors are separated by an approximate distance of 2.5 m. Power is coupled out of the laser through the ZnSe partially reflective flat mirror. The mirror assemblies and the laser plasma tube are supported by a four rod structure as can be seen in Figure 3.4.

The plasma tube is constructed from Pyrex and features an 18 mm inner bore and a 38 mm diameter water cooling jacket. There are two anodes at the ends and a cathode at the midsection of the laser plasma tube. One central gas inlet and two outlets are used to ensure a uniform gas flow throughout the amplifying region. Two rectangular ZnSe windows are mounted at a Brewster angle of 67.4°

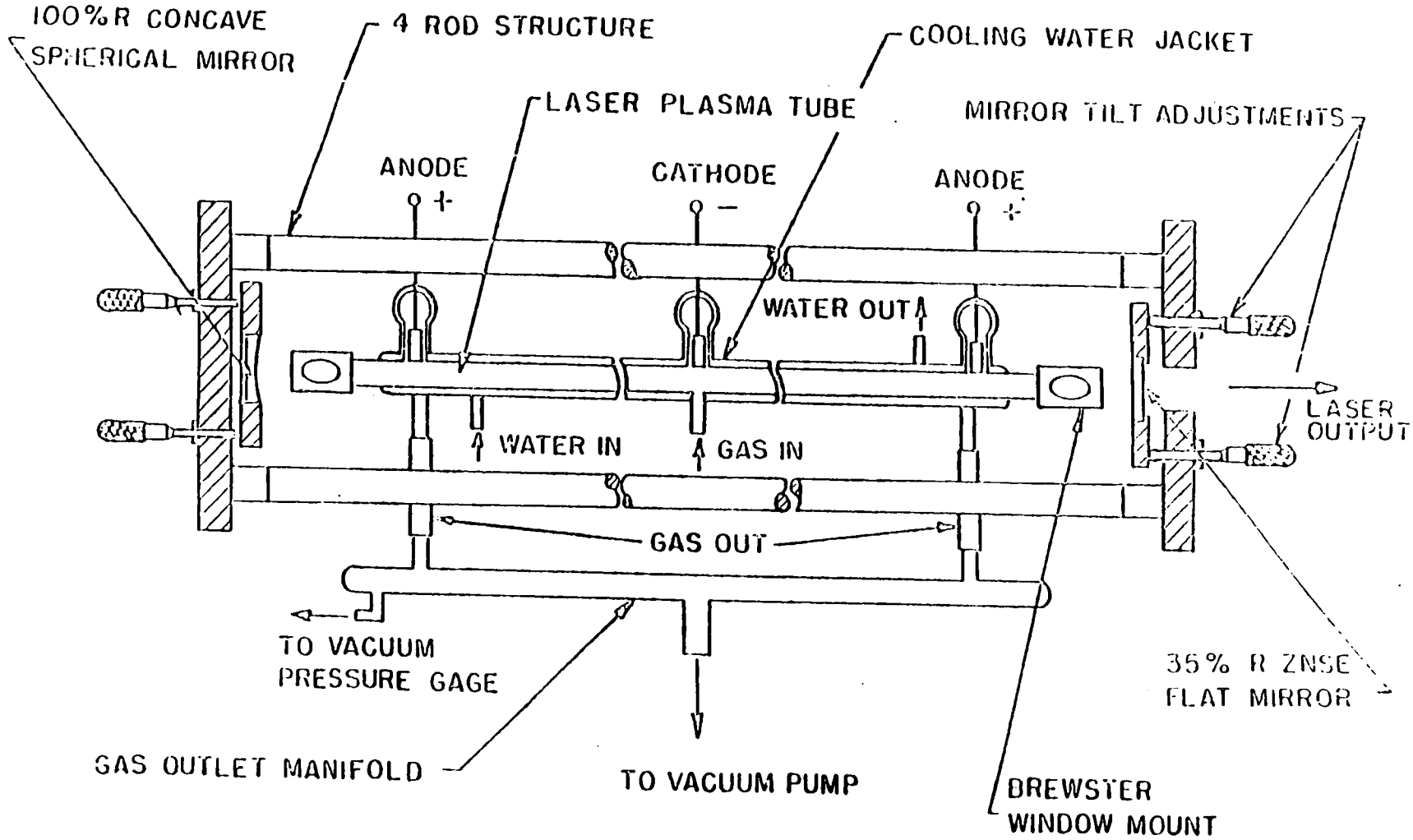

FIGURE 3.4 Top View of Laser Optical Resonator, Laser Plasma Tube and Mechanical Structure of CO_2 Laser

at the end of the laser plasma tube. At this Brewster's angle, there is no reflection of the transmitted electric field in the plane of incidence; therefore, the output of the CO_2 laser power in this design is linearly polarized in the vertical direction.

The gases are premixed in a chamber and by using a vacuum pump, the gases are drawn through the laser plasma tube. For effective operation of the CO_2 laser, a mixture of 80% helium, 15% nitrogen, and 5% CO_2 is used.

A Universal Voltronics power supply(20 KV, 100 mA) is employed to excite the gas mixture. The maximum power of the CO_2 laser is obtained at a discharge current of 70 mA. For safety precaution a number of switches and relays are installed to ensure that the laser does not operate should the laboratory door be opened inadvertently.

3.4.3 NEAR INFRARED TWO-COLOR PYROMETER

A fast response two-color pyrometer was employed to measure the surface temperature of the aluminum agglomerate. The function of the two-color pyrometer can be briefly described as follows: the radiation emitted from the burning droplet, is focused toward the bifurcated fiber optic cable by means of a zoom lens and the mirror M (see Figure 3.5). The bifurcated fiber optic cable then splits the transmitted beam into two beams which are directed into the detector housings D_1 and D_2. Before reaching the detector housings,

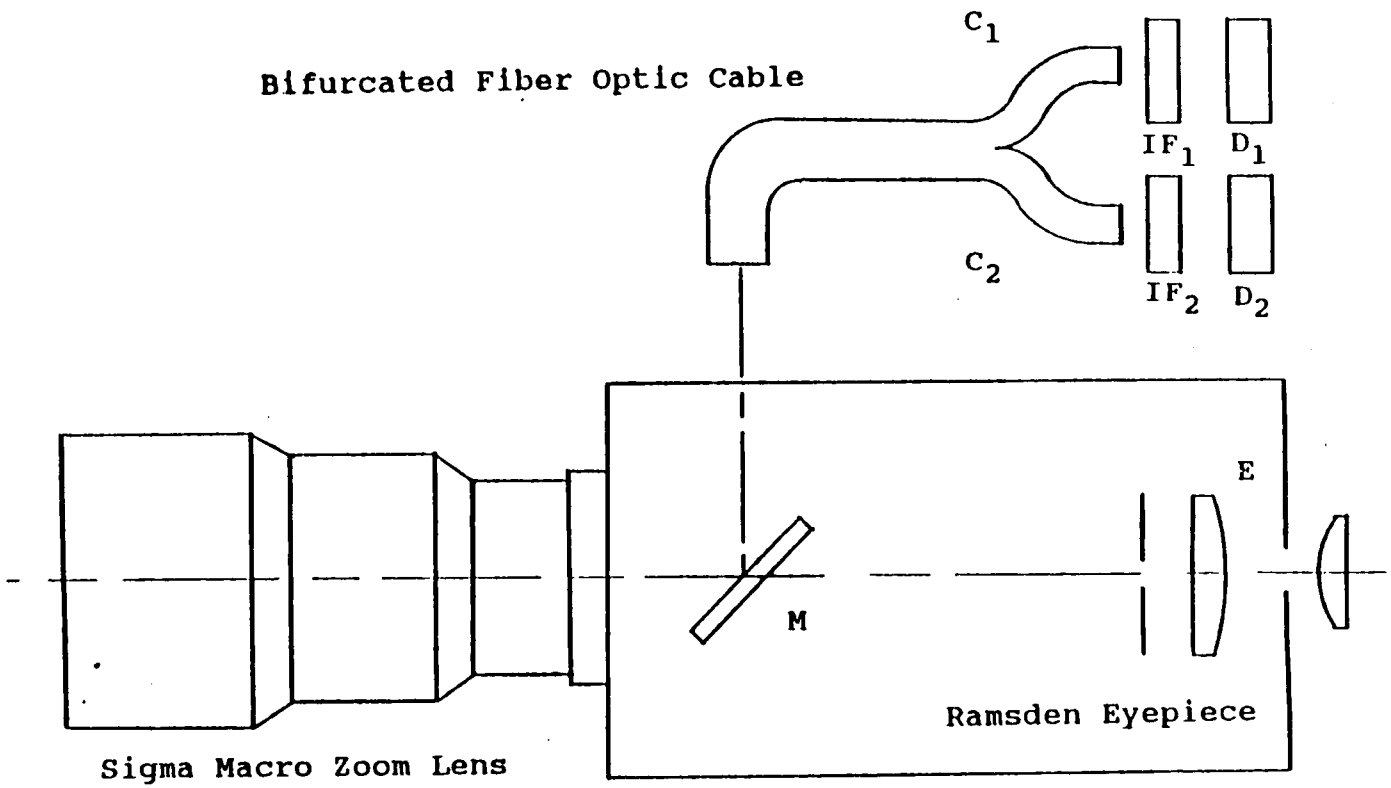

FIGURE 3.5 Schematic Diagram of the Optical Arrangement of Two-Color Pyrometer.

the two beams pass through interference filters IF_1 and IF_2, respectively. The two interference filters IF1 and IF2 are centered at 0.8 and 1.0 μm, respectively

Prior to each experiment, the pyrometer is precisely aligned to the agglomerate by focusing the agglomerate's image at the cross hair of the wide field of the ramsden eyepiece. The mirror, M, is then lowered to direct the emitted radiation of the agglomerate to the common leg of the fiber optic cable.

3.4.4 BROAD BAND RADIOMETER

A broad band radiometer is used to record the radiation emitted by the burning aluminum agglomerate. The radiometer's design is similar to that of the two-color pyrometer. Since no interference filters were used in the optical path, the radiometer is sensitive to broader radiation spectrum than the two-color pyrometer

3.4.5 HIGH-SPEED CAMERA

A Hycam model K2004E-115 16 mm motion picture was employed to record the ignition and combustion events for selected test runs. When the camera is used on a test run, the shutter and the data acquisition system are triggered after approximately 25 feet of the 100 foot film roll have been exposed. This permits the camera to

reach a steady-state speed when it starts filming the combustion event. Red dots were produced on the film by connecting the the red strobe light in the camera to a timer, preset at a 1 KHz frequency. This gives an accurate correlation between the filmed events and the output results obtained from the radiometer and pyrometer.

3.5 EXPERIMENTAL PROCEDURE

The experimental procedure is briefly described in this section. Prior to the experiment, the pyrometer is calibrated to account for any electronic drift caused by the temperature fluctuation over a period of time. The vacuum pump for the CO_2 laser is then turned on to evacuate the plasma tube before initiating the ionizing gas flow (He, N_2, CO_2).

After the CO_2 laser is activated, the laser beam is adjusted in order to obtain a bright and uniform laser beam (i.e, a Gaussian distribution). This is accomplished by adjusting the Zn-Se partial reflector such that it is parallel to the gold coated copper mirror (see Figure 3.4). The laser power can be varied either by varying the CO_2 flow rate or the current of the power supply or both.

The alignment of the CO_2 laser beam with the agglomer- ate is achieved by using a He-Ne laser. The He-Ne laser is introduced into the path of the CO_2 laser path by using a ZnSe beam splitter (F1). To ensure the CO_2 laser beam is irradiating both sides of alum-inum agglomerate, the following verifications are made prior to each

experiment. A plastic strip is mounted inside the combustion chamber; and mirror adjustments (M1, M2 and M3) are made until a rounded hole is obtained when the CO_2 laser irradiates the plastic strip. Once this is accomplished, the He-Ne laser beam is directed through the center of the hole. After the laser is aligned, the probe-supported aluminum agglomerate is mounted inside the combustion chamber.

The two-color pyrometer, the radiometer and the high-speed camera are aimed toward the agglomerate by centering the agglomerate's image at the crosshair graticules on the eyepiece of each instrument. The combustion chamber is then evacuated before pressurizing it with oxygen and nitrogen.

Finally the data acquisition system is set to the desired sampling rate. Then, the two-color pyrometer, the radiometer, the data acquisition system are activated by manually triggering the beam blocker or starting the high speed camera, if used in a test run. After a successful combustion test, a superimposed plot of the surface temperature and the relative radiation appear on the monitor; and the data are saved on the hard disk for future analysis.

3.6 DATA ACQUISITION SYSTEM AND ANALYSIS

The output voltages from the the two-color pyrometer and the radiometer are logged into an IBM PC system through a Metrabyte dash 16 A/D converter system. This system has the capability to

sample at a rate of 50,000 samples per second.

The data acquisition system is activated either by the shutter time or by the high-speed camera when the latter is used in a test run. The data are collected in terms of the output voltage as a function of time. Because of the mechanical lag time in the shutter mechanism, there is a deadband at the beginning of each data set collected from the pyrometer and the radiometer. This deadband is found to be approximately 40 ms. The data are then processed by a conversion program and stored in the hard disk for future analysis. The radiometer data is normalized so that the the stored data will be the relative intensity of the emitted radiation as a function of time. For the pyrometer data, a calibration equation is used to give the surface temperature of the aluminum agglomerate. The determination of the ignition delay time, the burning time and the surface temperature of the aluminum agglomerate will be discussed later.

In this study, aluminum agglomerates with nominal diameter of 535 μm were ignited at pressure between 0.1 and 4.3 MPa. For each pressure, a minimum of 10 test runs were performed to minimize the inherent error. Experimental data were eliminated either because of unsuccessful experiment (i.e, fiber consumption) or because the data did not satisfy the Chauvenet's criteria for statistical analysis [16]. Chauvenet's criteria basically eliminates a data point if the probability of obtaining the particular deviation from the mean is less than 1/2n where n is the number of data points in the set.

CHAPTER 4
EXPERIMENTAL RESULTS AND DISCUSSION

The ignition and combustion of laser-ignited aluminum agglomerates were studied as a function of ambient pressure. The experimental results are presented in this chapter. Aluminum agglomerates of nominal diameter 535 μm were mounted inside a high pressure combustion chamber and ignited by a focused CO_2 laser pulse. These experiments were performed at pressures between 0.1 and 4.3 MPa in a quiescent O_2/N_2 (20/80) atmosphere. A two-color pyrometer and a broad band radiometer were employed to measure the surface temperature and the droplet radiation, respectively. The combustion events were recorded by using high-speed camera. Section 4.1 presents the experimental observations and detailed discussions of the ignition and combustion behavior of aluminum agglomerate. Section 4.2 discusses the effects of pressure on the burning characteristics of aluminum agglomerate.

4.1 GENERAL OBSERVATIONS

This section is organized into three different subsections to facilitate the analysis of the ignition and combustion behaviors of aluminum agglomerate over the whole pressure range. These subsections include: low pressure regime (0.1 to 0.5 MPa), medium pressure regime (0.8 to 2.2 MPa) and high pressure regime (2.2 to

4.3 MPa).

4.1.1 LOW PRESSURE REGIME

In this regime the pressure ranges between 0.1 and 0.5 MPa. Figures 4.1.a and 4.1.b represent the radiation intensity and surface temperature curves at 0.5 MPa, respectively. The laser pulse for this particular experiment is 90 ms. The photographs in Figure 4.1.a show the four prominent stages that have been observed during ignition and combustion of aluminum agglomerate.

In this study the ignition delay time is defined as the time elapsed between the exposure of the agglomerate to the laser beam and the first appearance of the flame, which defined as the ignition point. Therefore, stage I in Figure 4.1.a represents the ignition delay time. It should be noted that the small segment (30 ms) preceding stage I is due to the mechanical lag of the beam blocker. During stage I, the agglomerate starts heating up as it is being irradiated by the CO_2 laser beam. This stage is characterized by the increasing change of the agglomerate's color to dark red (see photograph a). Because of the oxide layer, formed around the heated agglomerate, aluminum agglomerate does not ignite instantly as in the case of boron agglomerate [17]. The high melting temperature of aluminum oxide (2315 K) enables this oxide layer to maintain the integrity of the molten aluminum droplet. Furthermore, the impermeability of the oxide layer [2] slows the transport of the oxidant to the surface,

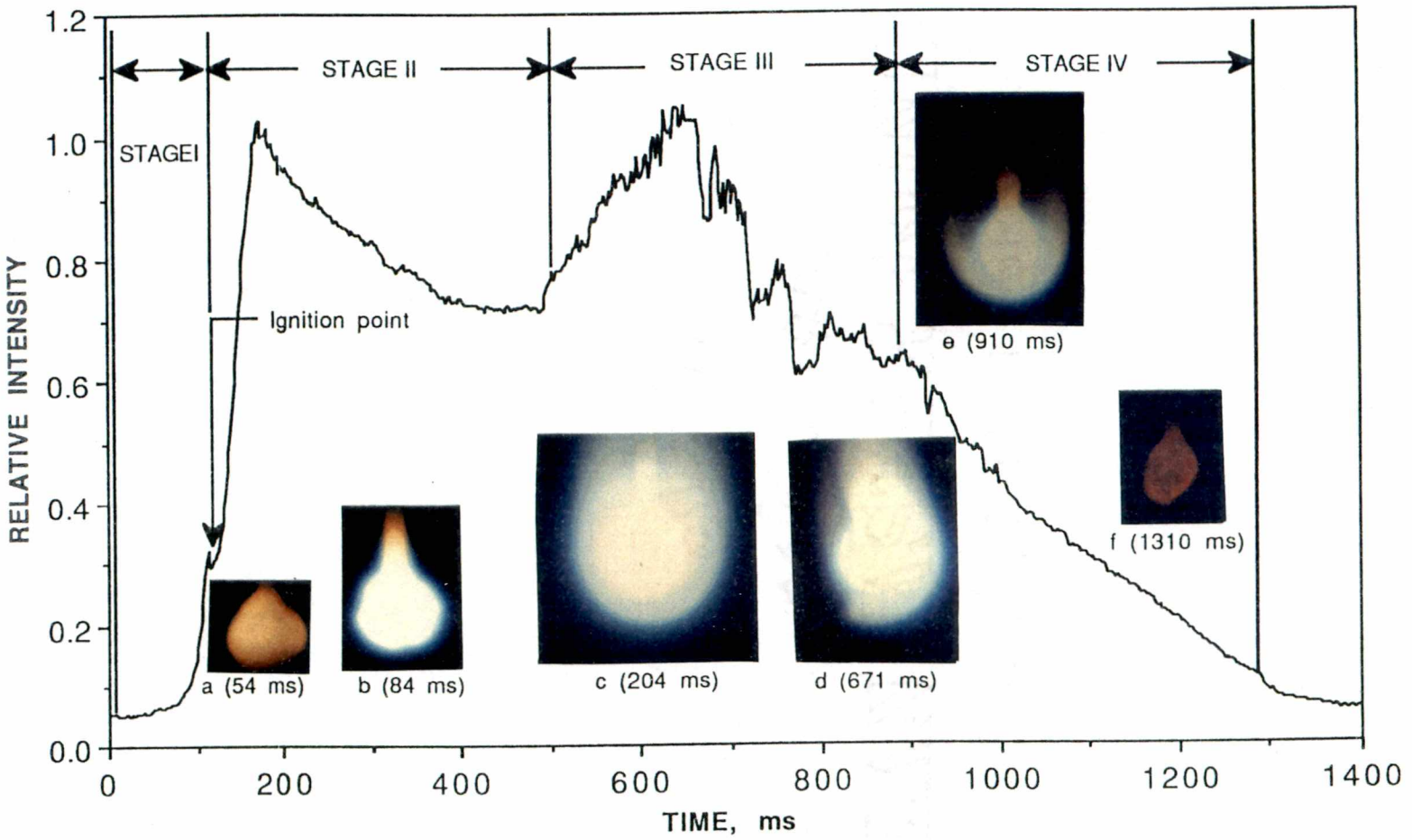

(a)

FIGURE 4.1 Typical Sequence of Events (a) and Surface Temperature Curve (b) of Laser-Ignited Aluminum Agglomerate at an Ambient Pressure of 0.5 MPa (Low Pressure Regime)

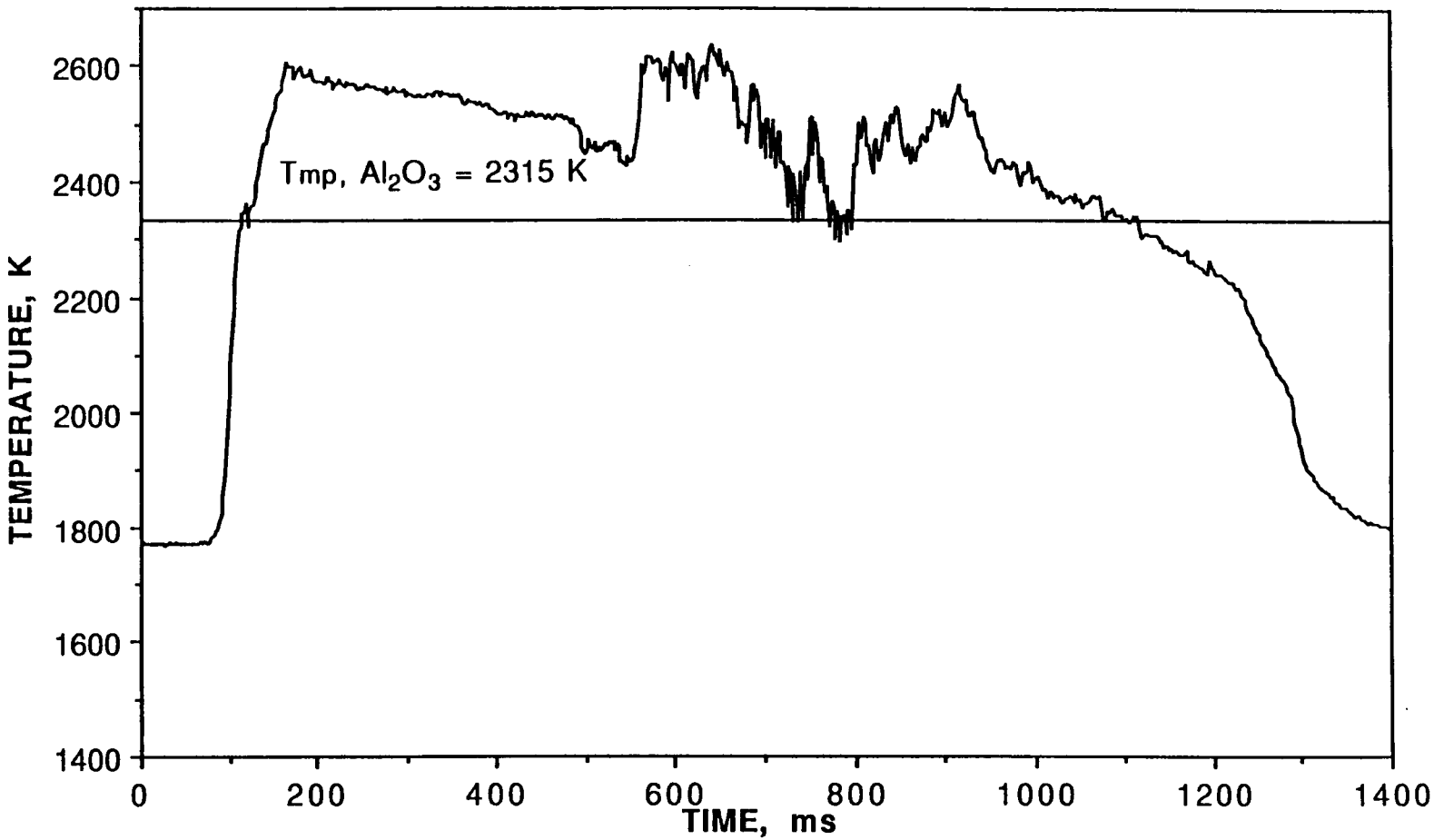

(b)

FIGURE 4.1 (Continued)

which makes aluminum hard to ignite. But as the agglomerate temperature rises, the oxide layer can no longer hold the molten droplet. The breaking up of the oxide layer was actually observed the film. The first appearance of the flame, defined as the ignition point, is characterized by very thin blue and violet zones. Interestingly, the ignition point corresponds to the first peak in the radiation curve (see Figure 4.1.a). This peak has been observed at all ambient pressures investigated in this study. From the surface temperature curve(4.1.b) the ignition point occurs at a temperature around 2319 K, which corresponds the melting temperature of aluminum oxide. Friedman and Macek [6,7] also noticed that the ignition occurs at the melting point temperature of aluminum oxide. In this particular experiment, the ignition delay time is approximately equal to 84 ms.

After the first appearance of the flame, a sudden increase in the radiation intensity and the flame size marks the transition from stage I to stage II. The sudden increase in the radiation intensity can not be due to the laser since it was shut off few milliseconds before the flame expansion. Friedman [6] also observed this sudden increase of intensity and he attributed it to the ignition characteristics of aluminum. The flame then stabilizes around the droplet with a distinctive green envelope surrounded by a thin blue zone (see photograph b). The flame is located at a distance away from the droplet; and as discussed by Davis [1] this flame structure suggests a vapor-phase reaction. The observed green-blue envelopes is the characteristics of AlO spectrum [18,19]. In this stage the flame

appears to be spherically symmetric. The combustion is steady and no fragmentation nor droplet movement are observed in this stage. Because the radiation emitted in this regime is not so intense, the molten droplet can be clearly observed on the film. A typical flame structure in this stage is shown in Figure 4.2 where the molten droplet is surrounded by a white zone and then by a green-blue envelope. The vapor oxide, observed at the upper part of the flame, is naturally convected in the cooler wake region and condensed on the SiC fiber.

The second stage of this regime starts with particle fragmentation. In this regime, the fragmentation is very weak and relatively more fragmentations are observed at atmospheric pressure than that at 0.5 MPa. The flame structure is no longer symmetric and frequent movements of the droplet was observed. In this stage more oxide is convected upward. Since the emitted radiation is not so intense in the low pressure regime, especially at 0.1 MPa, the formation of the oxide layer on the leeward side of the droplet surface is actually observed on the films. This shell of oxide is floating around the molten droplet from one side to another and finally settled in the bottom side of the droplet. Wong and Turns [14] also observed the formation of the cap oxide on the leeward side the droplet. It appears that in this the oxide condensation at the droplet surface is responsible for the fragmentation and the frequent movements of the droplet. Prentice [10] attributed the unsteady behavior of the aluminum droplet burning to the oxide accumulation

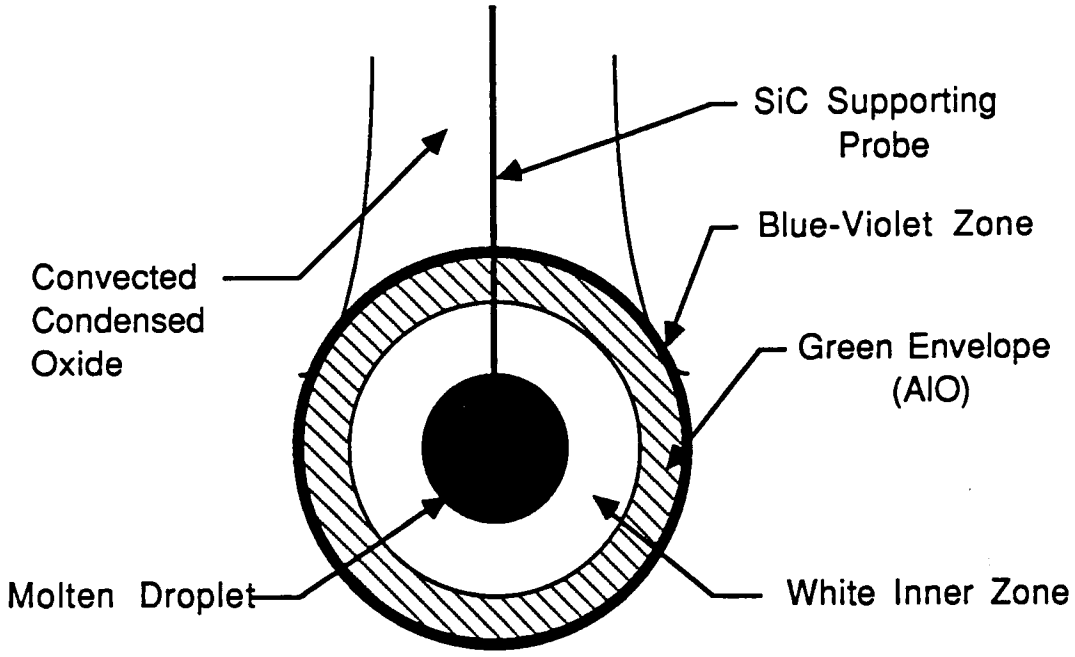

FIGURE 4.2 Typical Flame Structure at Low Pressure Regime

on the droplet surface.

The final stage of this regime is marked by the ending of the droplet fragmentation and the decaying of the flame size with a noticeable decrease in size of the green zone (see photograph d). In this stage the burning is more stable than in stage II. The flame continues to decrease until it becomes localized on one side of the droplet surface where the vapor fuel is still diffusing out to react with oxygen. Finally, the flame collapses on the condensed oxide and no more vapor is observed on the film. At this point the combustion is assumed to be completed. Therefore, the burning time is defined as the time elapsed between the ignition point and the instant at which no more vapor oxide is observed. For this particular experiment the burning time was found to be 1220 ms.

Figure 4.3 is a photograph of the combustion residue at an ambient pressure of 0.1 MPa. The condensed oxide can be seen in the upper part of the SiC fiber which is being coated by white aluminum oxide powder. The combustion product contains a small residue of unburned aluminum metal. The unburned metal existed because at the end of the burning stage, the low temperature gradient is not able to drive the aluminum vapor outwardly to react with oxygen. Turns and Wong [14] also observed that at low ambient gas temperatures (<= 1580 K) the combustion product also contains small residue of unburned aluminum metal.

Figures 4.4.a and 4.4.b show typical radiation intensity and surface temperature curves at 0.1 MPa, respectively. The surface

FIGURE 4.3 Typical Combustion Products at an Ambient pressure of 0.1 MPa (Low Pressure Regime).

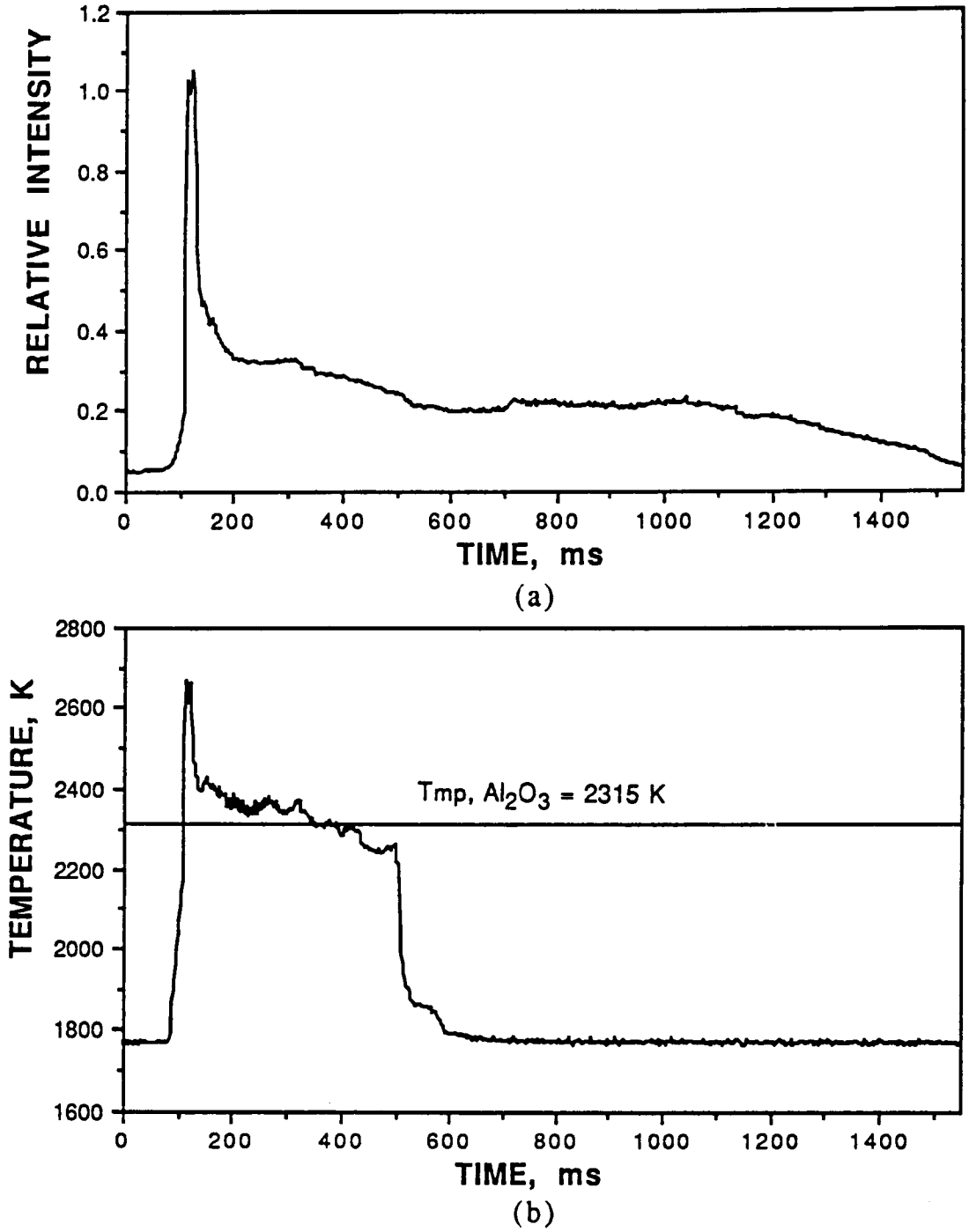

FIGURE 4.4 Typical Radiation Intensity Curve (a) and Surface Temperature Curve (b) of a Laser-Ignited Aluminum Agglomerate at an Ambient Pressure of 0.1 MPa.

temperature curve in Figure 4.4.b does not reflect the different stages of the combustion events since the temperature decreases abruptly at 400 ms after ignition. This is due to the fact that right after ignition the aluminum droplet moved to one side of the SiC fiber; and consequently, only the hot SiC fiber is exposed to the target of the pyrometer. At atmospheric pressure the aluminum agglomerate ignites and burns in a similar fashion as that at 0.5 MPa with only few exceptions. First, sporadic fragmentations occur more frequently at atmospheric pressure than that at 0.5 MPa. Second, the emitted radiation from the droplet is less intense at 0.1 MPa than that at 0.5 MPa. Therefore, during stage III of the combustion event at atmospheric pressure, the formation of the oxide cap on the leeward side of the aluminum droplet can be seen clearly on the film record.

At atmospheric pressure the average burning time (for 10 experimental data points) is 1338 ms. The burning time obtained by Wong and Turns [14] is approximately 680 ms. The discrepancy between these two values can be explained by the fact that in the present study the experiments were performed in cold gas environment. On the other hand, Wong ant Turns performed their experiments in a hot gas environment.

4.1.2 MEDIUM PRESSURE REGIME

In this regime the experiments were performed at pressures

between 0.8 and 1.5 MPa. Figures 4.5.a and 4.5.b show typical radiation intensity and surface temperature curves of the ignition and combustion of aluminum agglomerate at 0.8 MPa. The photographs in Figure 4.5.a show the four different stages of the combustion.

According to the definition of the ignition delay time used in this study, stage I in Figure 4.6.a represents the ignition delay time. The ignition point, shown in photograph b in Figure 4.6.a, corresoponds to a steep change in the radiation intensity curve. From the surface temperature curve (see Figure 4.6.b), the temperature at ignition is 2406 K, which is in the neighborhood of the melting temperature of aluminum oxide (2315 K). At its first appearance, the flame surrounds the agglomerate uniformly (see photograph b) and is characterized by a blue-violet thin zone. For this particular experiment, the ignition delay time is 102 ms, which is comparable to that for the low pressure regime.

The transition from stage I to stage II is marked by the expansion of the flame's size and an increase of the emitted radiation intensity. The increase in the flame size and the droplet luminosity are due to the melting of the oxide layer and the diffusion of the aluminum vapor fuel. After a few milliseconds, the flame stabilizes around the droplet. The flame is detached and symmetrically stable around the droplet (see photograph c). The symmetry of the upper part flame is disturbed by the the convected smoke. The flame structure, as shown in Figure 4.6, consists of a white inner zone and a thin blue-violet zone. Because of the intense luminosity, the outline

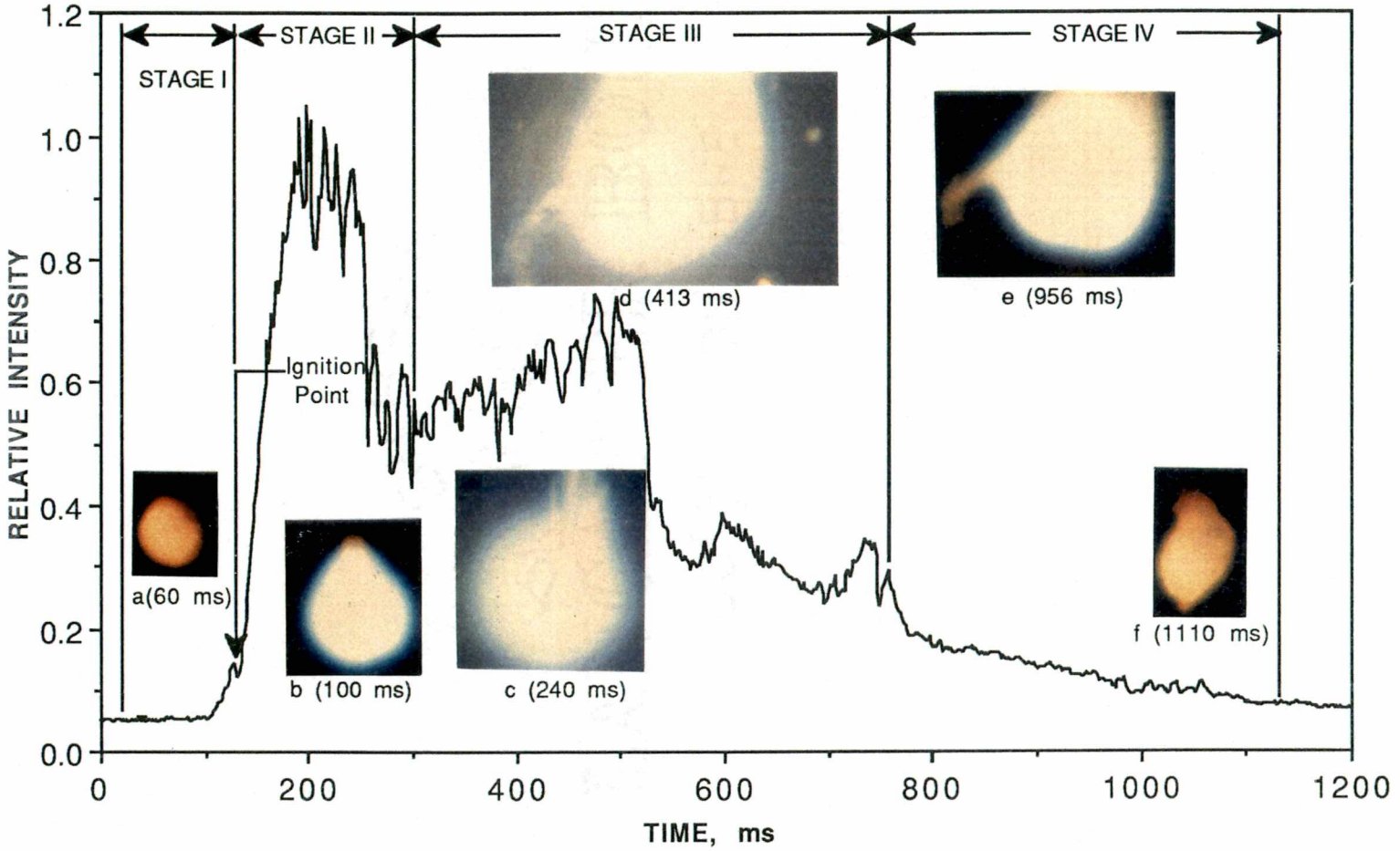

(a)

FIGURE 4.5 Typical Sequence of Events (a) and Surface Temperature Curve (b) of Laser-Ignited Aluminum Agglomerate at an Ambient Pressure of 0.8 MPa (Medium Pressure Regime)

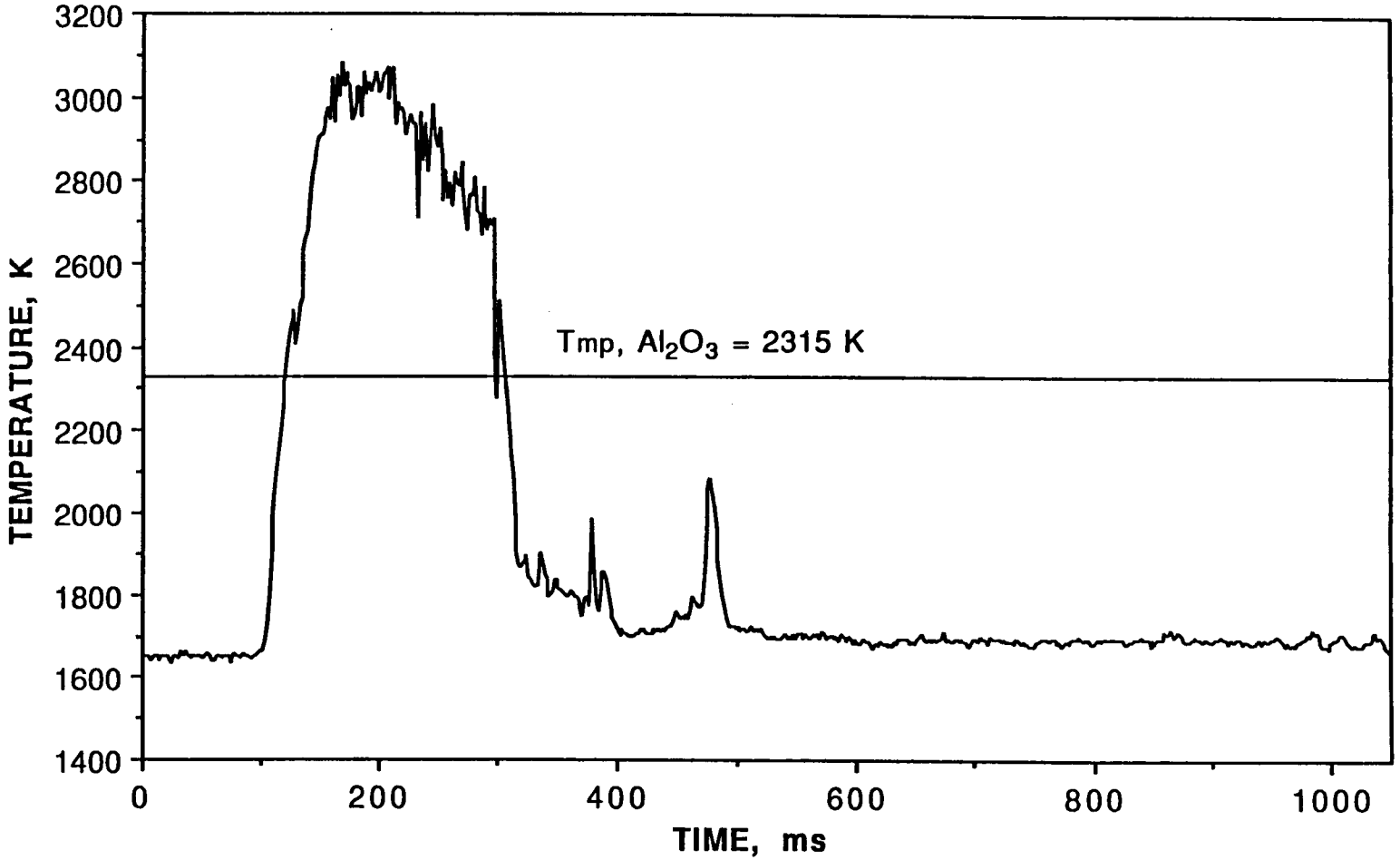

(b)

FIGURE 4.5 (Continued)

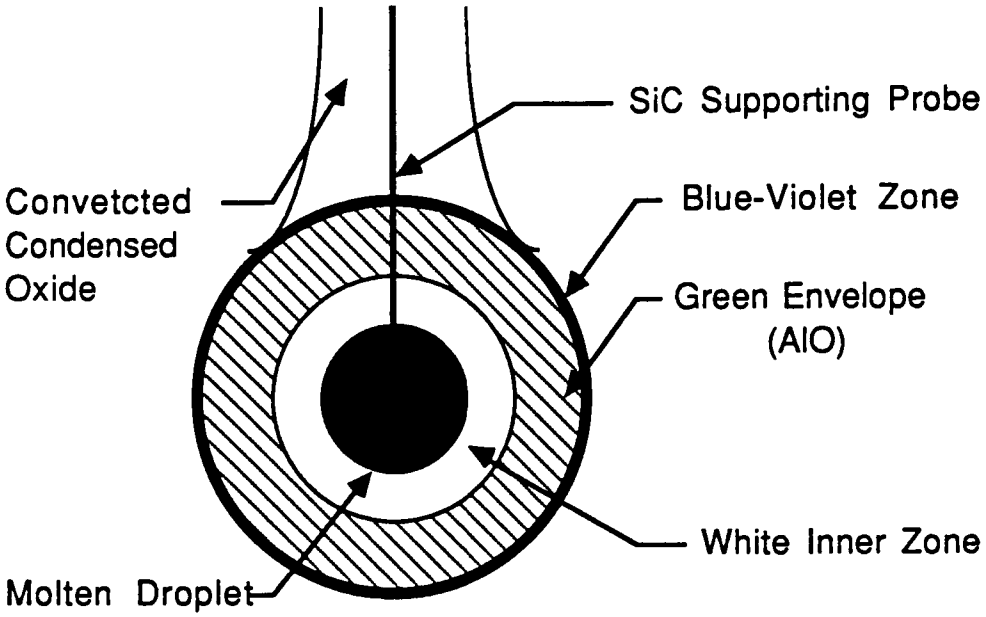

FIGURE 4.6 Typical Flame Structure at Medium Pressure Regime

of the molten aluminum droplet can not be discernible on the film record. The oxide vapor is convected upward in the cooler wake region. In this regime the flame front is much closer to the droplet surface than that in the low pressure regime.

Stage III starts with strong fragmentation and particle ejection in random directions as can be seen in photographs b in Figure 4.6.a. The flame symmetry is distorted and the thickness of the green envelope varies randomly. Furthermore, periodic changes in the droplet light emission are observed. This can be related to the droplet movement around the SiC fiber. Friedman [3] and Prentice [10] have noticed the droplet is spinning during aluminum combustion. The droplet is also observed to move up the fiber whose tip is consumed during combustion. As a result, the droplet moves out of view of the pyrometer's small target area; and the indicated temperature decreases abruptly to a low level (1740 K). Therefore, the surface temperature curve can be used to analyze only stage I and stage II of the ignition and combustion events of aluminum agglomerate.

The transition from stage III to stage IV is characterized by the end of fragmentation and droplet movement. The flame size (along with the green envelope) decreases continuously during stage IV. The droplet burning is relatively more stable in stage IV than in stage III (see photograph d). Decaying of the flame size continues until it becomes localized on one side where aluminum vapor fuel is diffusing out to react with oxygen. The flame then collapses on the

oxide surface which continues to glow (see photograph f); and finally no radiation is visible on the film record. The burning time for this particular experiment was determined to be approximately 1028 ms.

Figures 4.7.a and 4.7.b show the radiation intensity curve and the surface temperature at 1.5 MPa, respectively. The surface temperature in Figure 4.7.b does not correlate with the four combustion stages. This is due to the movement of the droplet during stage III as stated before. The ignition and combustion characteristics of aluminum agglomerates at 1.5 MPa are essentially the same as at 0.8 MPa. However, at 1.5 MPa the particle ejection and fragmentation in stage III are not as strong as at 0.8 MPa. For this particular experiment (1.5 MPa), the burning time was approximately 1013 ms which is less than that obtained at 0.8 MPa.

Figure 4.8 is photograph of a typical combustion residue in the medium pressure range. The condensed vapor oxide can be seen in the upper part of the SiC fiber. The product consists mainly of white aluminum oxide. Some samples of the combustion residue were sectioned and observed through the microscope, but this did not reveal any indications of unburned aluminum metal. The oxide product is nearly spherical and constitutes 80% of the parent agglomerate size.

4.1.3 HIGH PRESSURE REGIME

In this regime the flame is very close to the surface of the aluminum droplet. At high pressure, the droplet combustion is

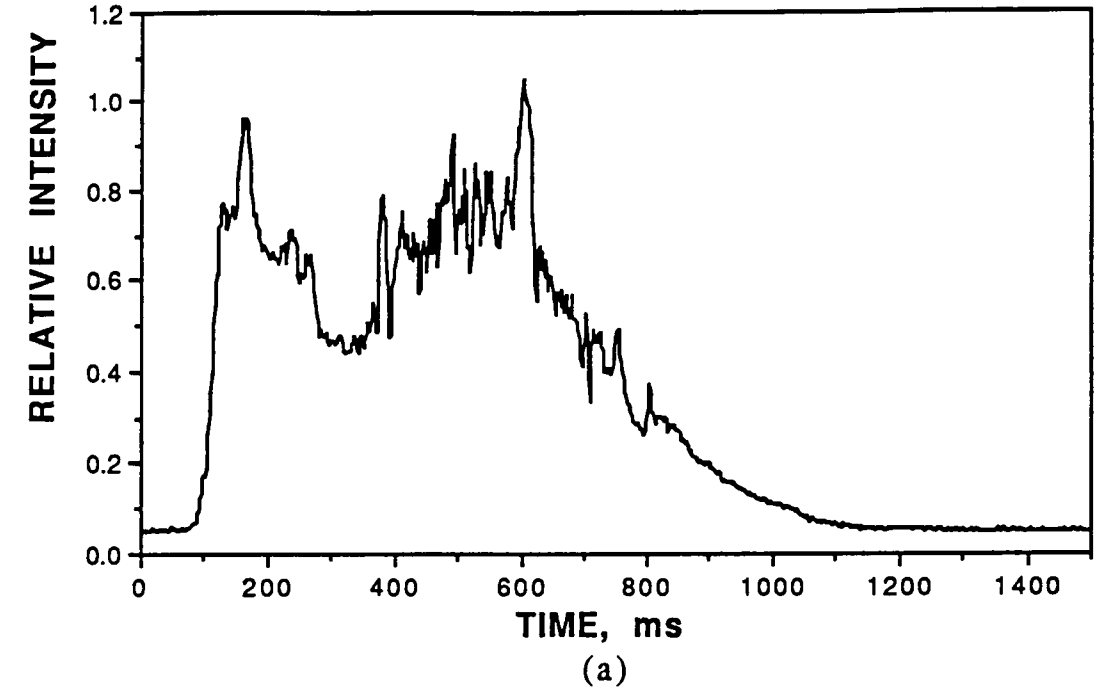

(a)

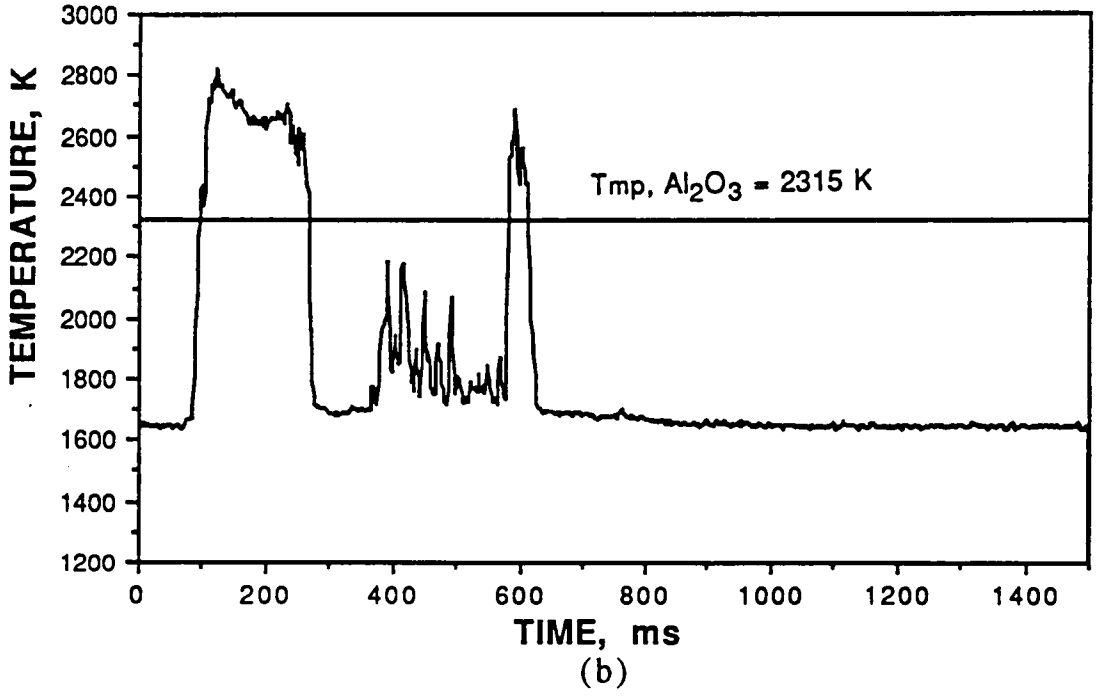

(b)

FIGURE 4.7 Typical Radiation Intensity Curve (a) and Surface Temperature Curve (b) of a Laser-Ignited Aluminum Agglomerate at an Ambient Pressure of 1.5 MPa

FIGURE 4.8 Typical Combustion Product at an Ambient Pressure of 0.8 MPa (Medium Pressure Regime)

similar to that of a hydrocarbon fuel droplet. The experiments in this regime were performed over a pressure range between 2.2 and 4.3 MPa. Figures 4.9.a and 4.9.b show typical radiation intensity and surface temperature curves at 4.3 MPa. The photographs in Figure 4.9.a depict the four prominent stages during combustion.

Stage I is the ignition delay time as defined in the present study. Photograph a in Figure 4.9.a shows the agglomerate during irradiation by the CO_2 laser beam. The flame at its first appearance; i.e., ignition point, uniformly envelopes the agglomerate with a blue-violet zone. The appearance of the flame corresponds to a change in the slope of the radiation curve (see photograph b). From the surface temperature curve in Figure 4.9.b, the temperature of the droplet at ignition is approximately 2424 K, which is in the neighborhood of the melting temperature of aluminum oxide. For this particular experiment, the ignition delay time was approximately 60 ms.

Stage II starts with increasing in both flame size and droplet luminosity. After few milliseconds, the flame stabilizes around the droplet whose resembles that of a hydrocarbon fuel droplet. The general flame structure in this stage is shown in Figure 4.10. The flame is characterized by a thick green envelope which is adjoined by a thin blue-violet zone. The flame is symmetrically close to the droplet surface. Davis [1] also noticed that at high pressure the aluminum particles burn like hydrocarbon fuel droplets. The vapor oxide convected in this stage is less than that in low and medium pressure regimes.

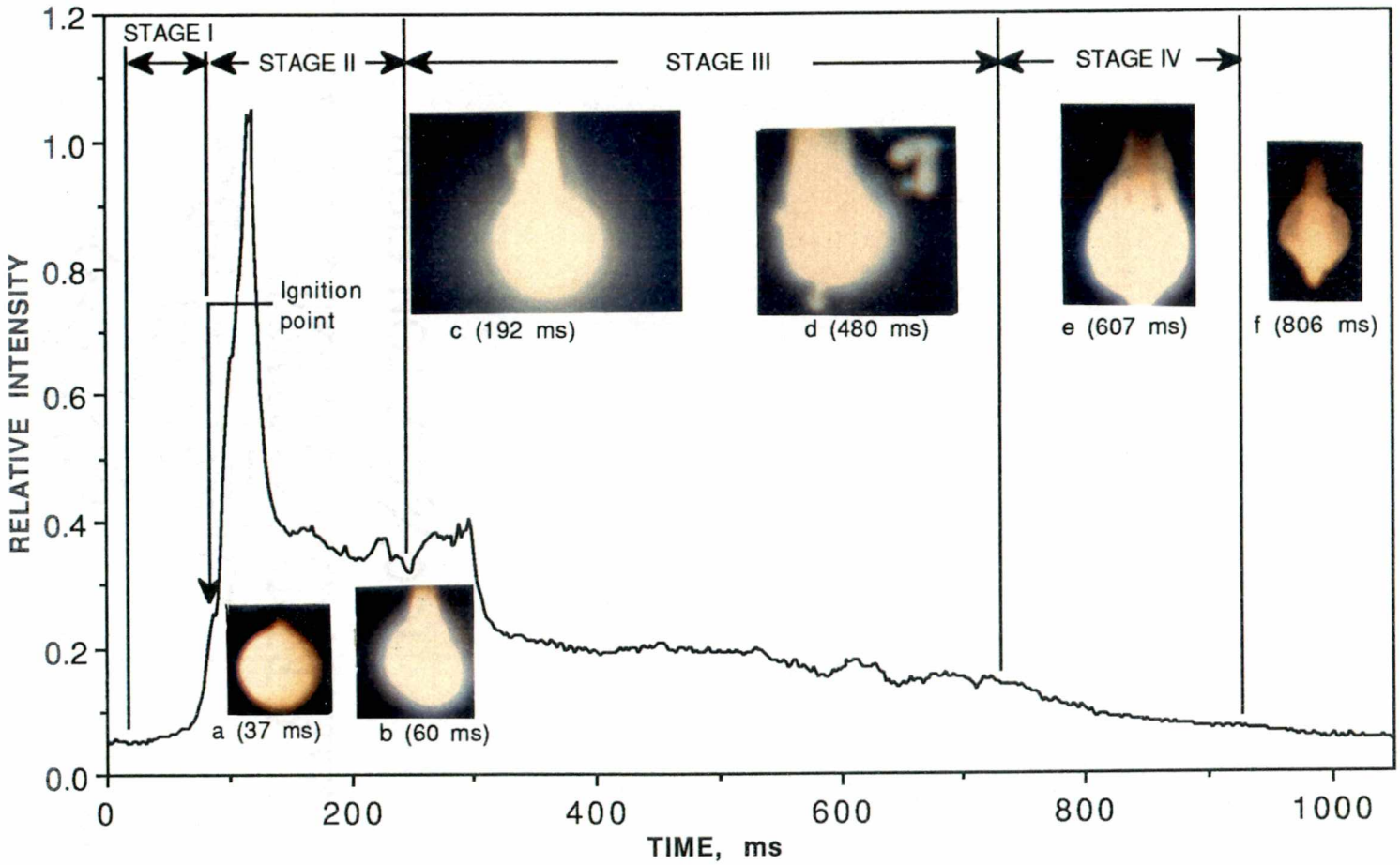

(a)

FIGURE 4.9 Typical Sequence of Events (a) and Surface Temperature curve (b) of Laser-Ignited Aluminum Agglomerate at an Ambient Pressure of 4.3 MPa (High Pressure Regime)

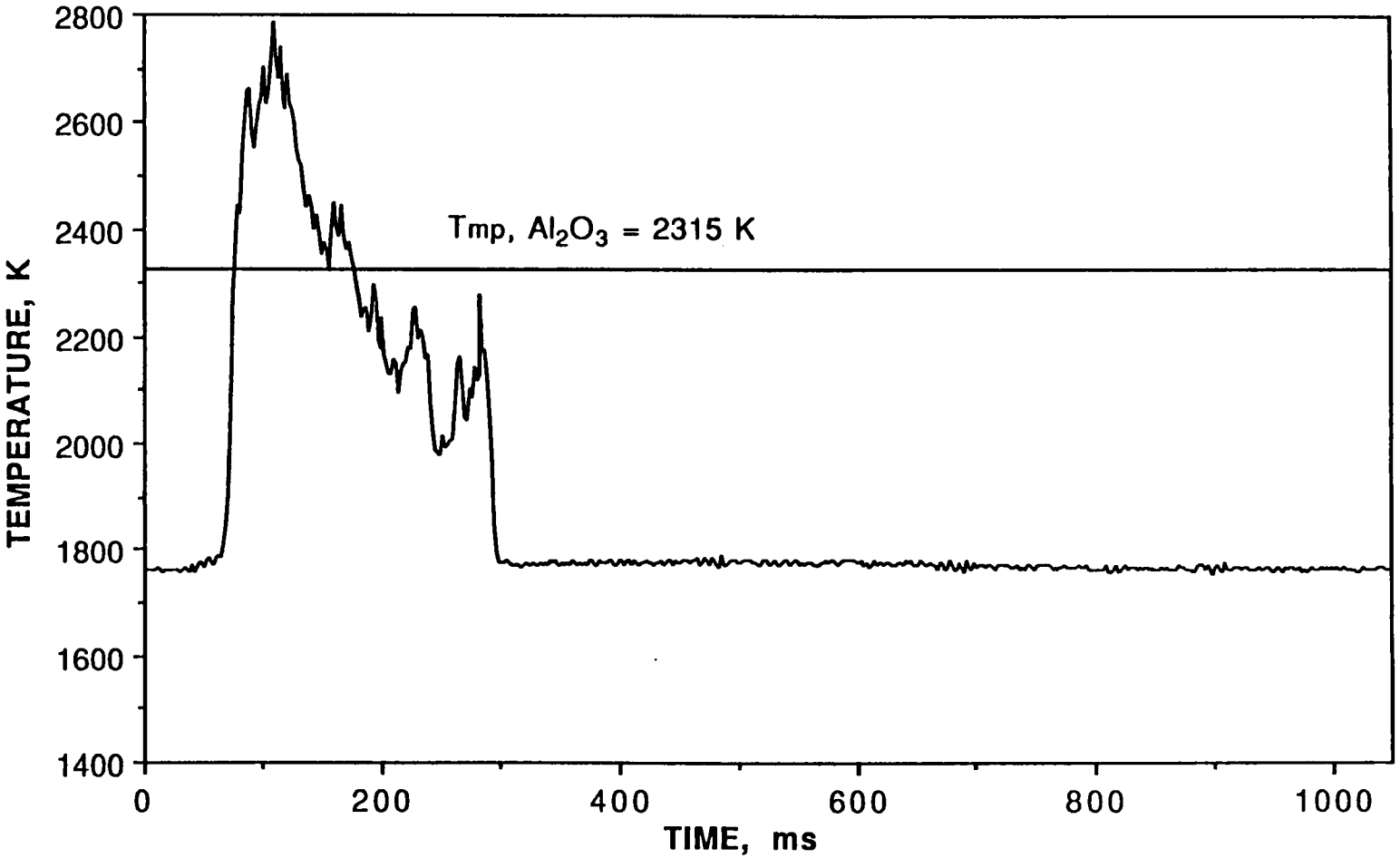

(b)

FIGURE 4.9 (Continued)

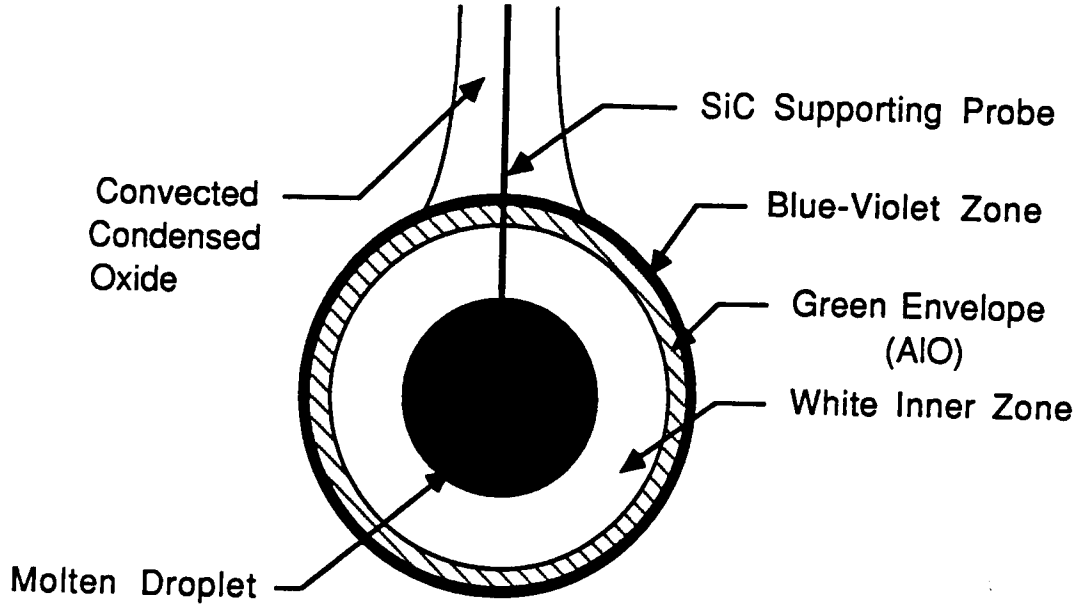

FIGURE 4.10 Typical Flame Structure at High Pressure Regime

Stage III starts with weak and sporadic particles' ejection in random directions. Vibrations and movements of the droplet around the SiC fiber are observed during this regime. Because of the high radiation intensity emitted from the droplet, specific details of either the molten droplet or the oxide formation were not available for observation on the film record. The flame is no longer symmetrical (see photograph c); and the thickness of the green envelope varies randomly. More oxide vapor is convected in this stage than in stage I of this regime. Because the molten droplet moves up on the SiC fiber and moves out of view from the target's of the two-color pyrometer, no surface temperature was recorded in this stage (see Figure 4.9.a). Therefore the surface temperature curve in Figure 4.9.b can be used to analyze only stage I and II of the combustion events.

In stage IV the combustion becomes steady with neither fragmentation nor movement of the droplet. The flame size which is symmetric around the droplet, starts to decrease along with is green envelope. Finally the flame becomes localized and then collapses on the oxide surface (see photograph d). For this particular experiment, the burning time was approximately 850 ms.

Figures 4.11 to 4.13 show typical radiation intensity and surface temperature curves at 2.2, 2.9 and 3.6 MPa, respectively. At these pressures, the ignition and combustion characteristics of aluminum agglomerates are similar to those at 4.3 MPa. These characteristics include: steady droplet burning, flame contiguous to the droplet surface, and weak droplet fragmentation.

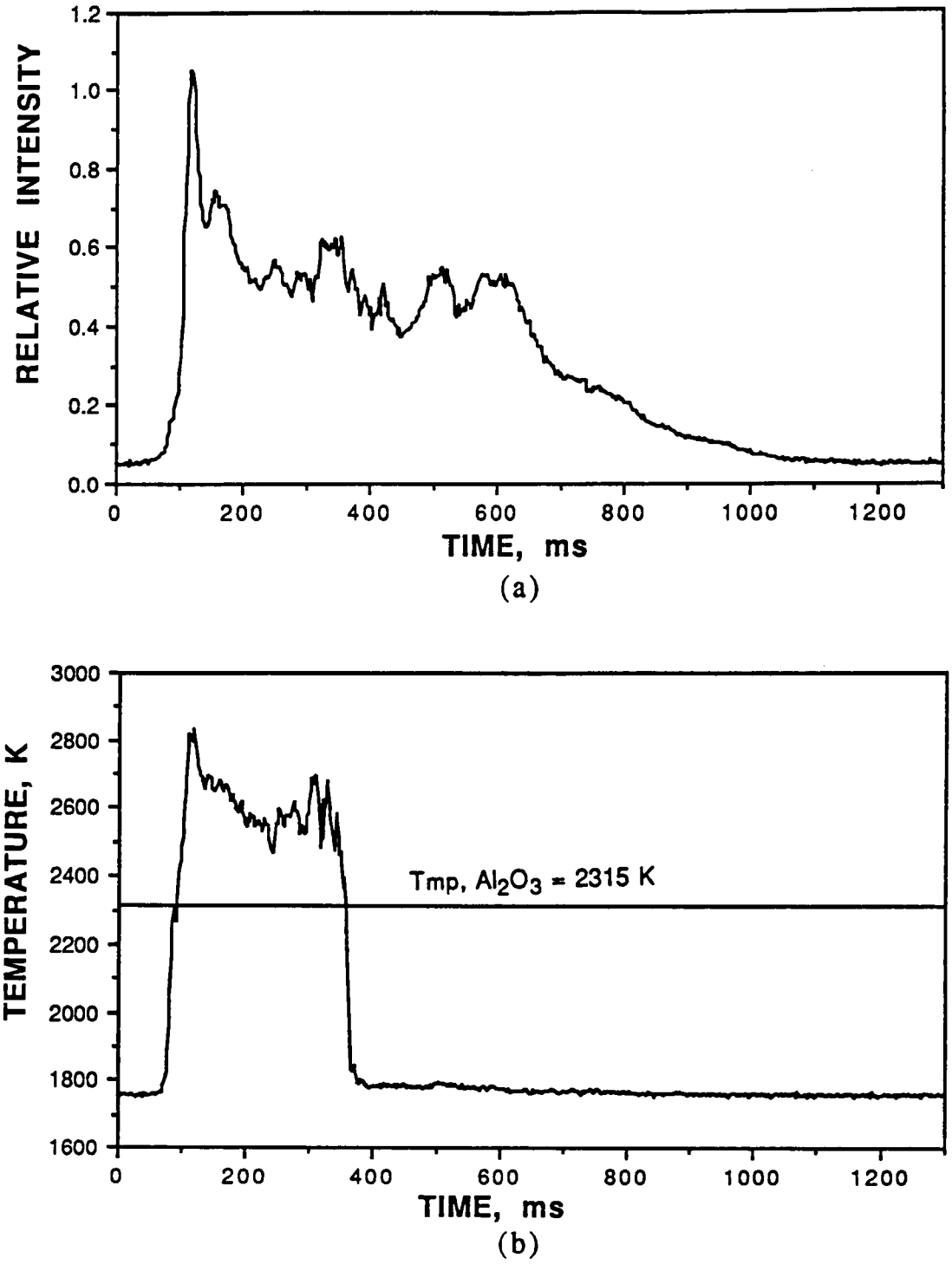

FIGURE 4.11 Typical Radiation Intensity Curve (a) and Surface Temperature Curve (b) of a Laser-Ignited Aluminum Agglomerate at an Ambient Pressure of 2.2 MPa

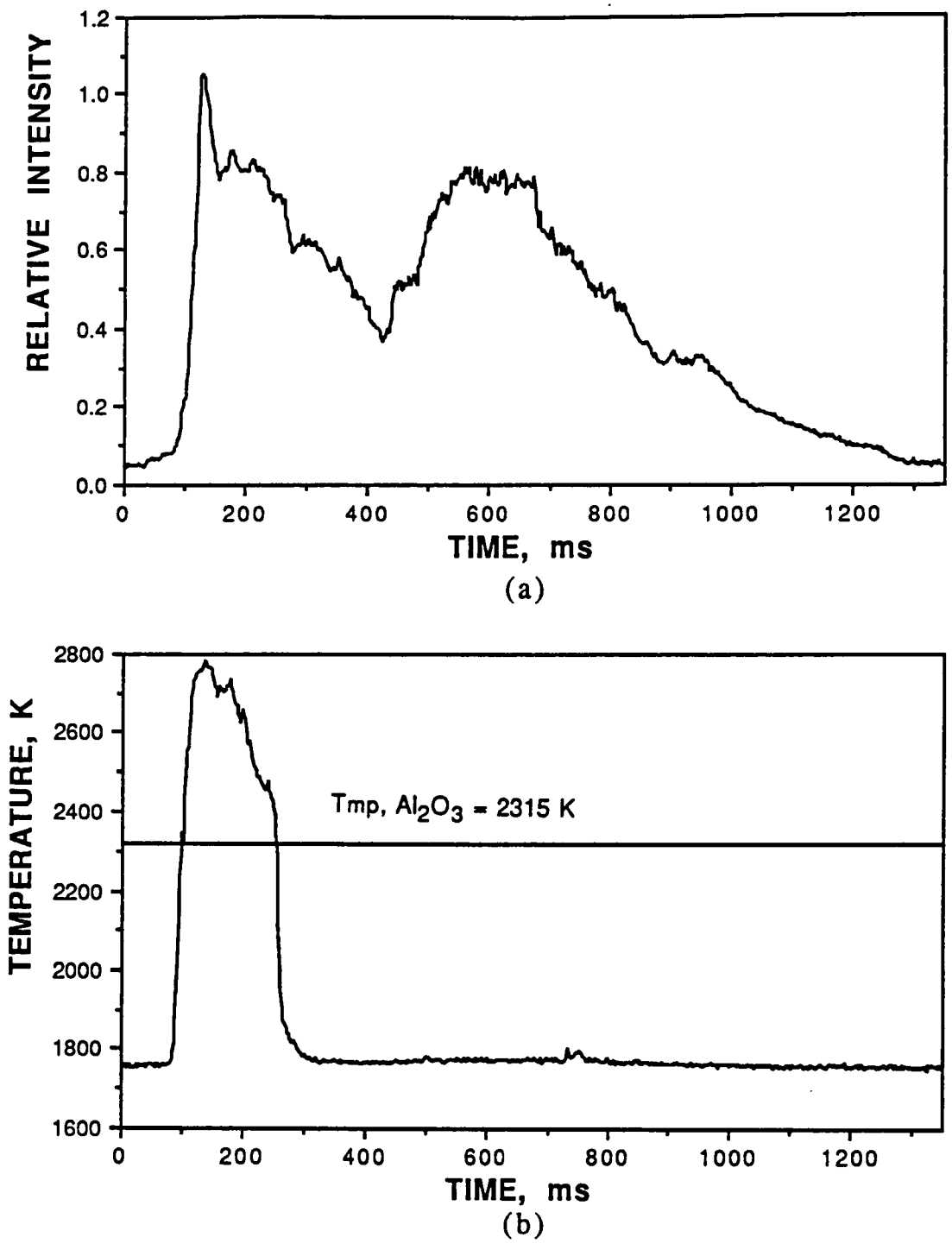

FIGURE 4.12 Typical Radiation Intensity Curve (a) and Surface Temperature Curve (b) of a Laser-Ignited Aluminum Agglomerate at an Ambient Pressure of 3 MPa

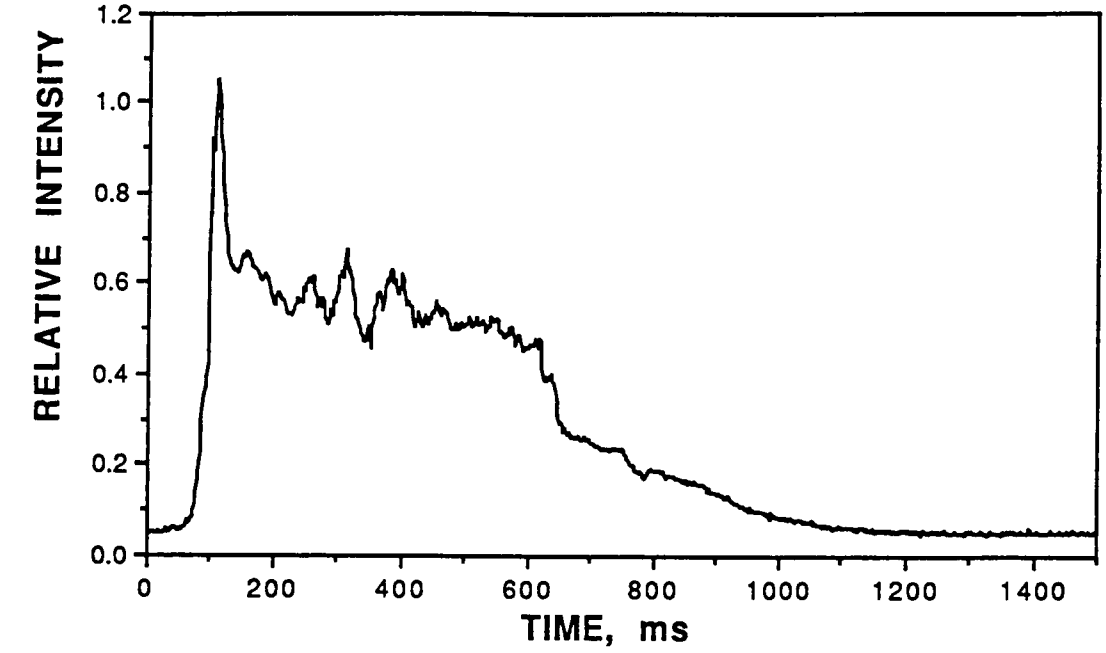

(a)

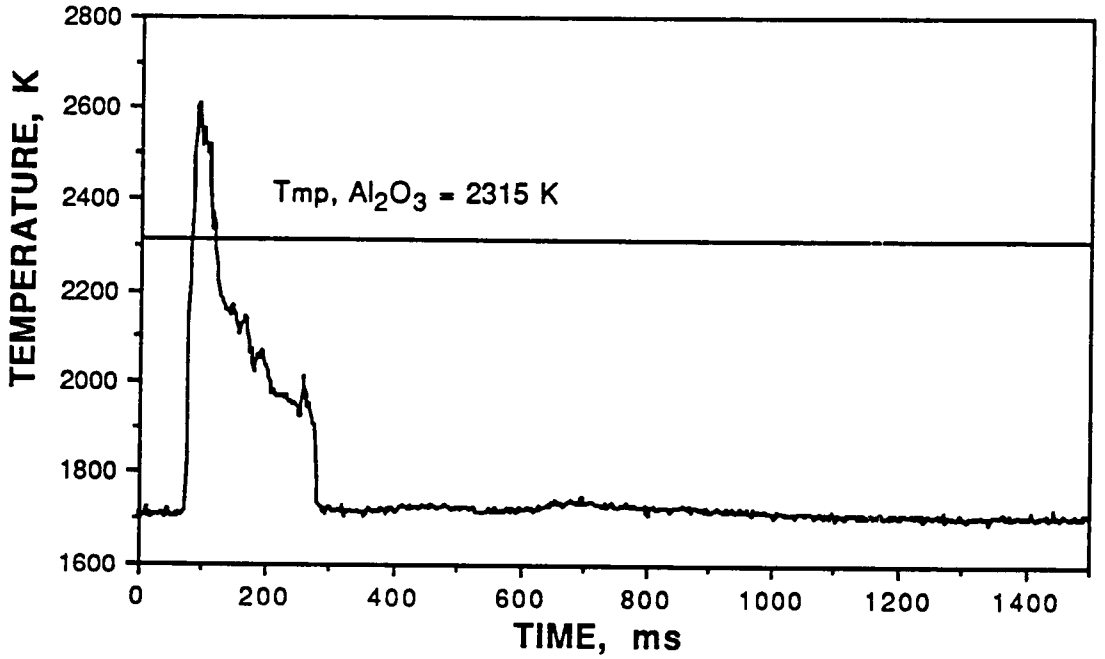

(b)

FIGURE 4.13 Typical Radiation Intensity Curve (a) and Surface Temperature Curve (b) of a Laser-Ignited Aluminum Agglomerate at an Ambient Pressure of 3.6 MPa.

Figure 4.14 is a photograph of a typical combustion residue obtained in the high pressure regime. The upper part of the SiC fiber can be seen coated by the condensed vapor oxide. The residue consists of white aluminum oxide, and represents 80 to 90% of the original size of the aluminum agglomerate. Observations of sectioned samples of the aluminum oxide residue through the microscope, revealed no trace of unburned aluminum metal.

4.2 EFFECTS OF PRESSURE

The effects of the ambient pressure on the ignition delay time, the burning time and the flame structure will be discussed in this section.

In the present study the laser pulse duration was maintained at 90 ms and the laser power was kept between 30.3 and 31.46 W. Table 4.1 shows the ignition delay time as a function of the ambient pressure. Results using the laser ignition technique indicate that the ambient pressure has no significant effect on the ignition delay time. This is thought to be due to the high radiation energy used to ignite the aluminum agglomerate. The ignition delay time varies between 55 and 80 ms with no obvious trend indicating the pressure effect.

Table 4.2 shows the effect of pressure on the burning time of aluminum agglomerate. The burning time decreases as the pressure increases; however, the burning time is more sensitive to pressure at

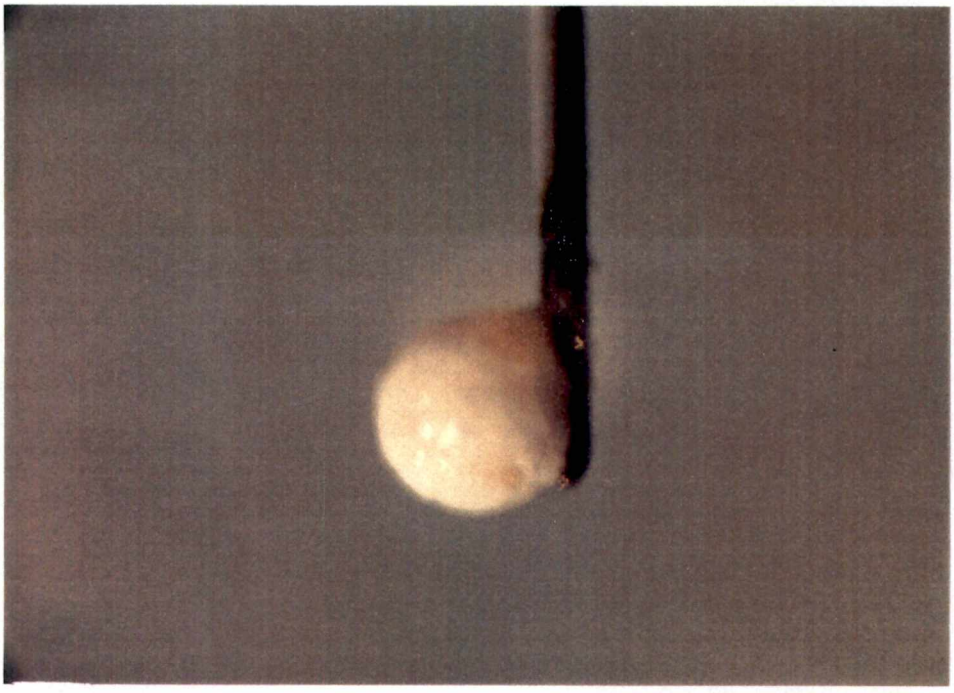

FIGURE 4.14 Typical Combustion Product at an Ambient Pressure of 4.3 MPa (High Pressure Regime)

TABLE 4.1 Effect of Pressure on the Ignition Delay Times

Pressure (MPa)	Ignition Delay Times (ms)
0.1	74
0.5	77
0.8	63
1.5	66
2.2	78
3.0	80
3.6	60
4.3	55

TABLE 4.2 Effect of Pressure on the Burning Times

Pressure (MPa)	Burning Times (ms)
0.1	1338
0.5	1248
0.8	1080
1.5	1005
2.2	950
3.0	949
3.6	959
4.3	895

low pressures than that at high pressures (see Figure 4.15). For example, at low pressure an increase of 0.4 MPa caused a decrease of 90 ms in the burning time. On the other hand, at high pressure increasing the pressure from 2.2 to 3.6 MPa decreased the burning time by only 9 ms. At low pressure (1-5 MPa) most of the vapor oxide was convected and condensed in the wake region; whereas at high pressure the vapor oxide diffused primarily inward and condensed on the droplet surface. The oxide accumulation has a strong effect on the burning mechanism of aluminum droplets in the medium pressure regime where strong fragmentation and droplet movement were observed (especially during stage III of combustion events). In the high pressure regime the oxide condensation does not have a strong effect on the burning mechanism; and except for sporadic fragmentation during stage III of the combustion event, aluminum agglomerates burn like hydrocarbon fuel droplets.

The flame radius moves closer to the surface as the ambient pressure increases. At low pressure the flame is located away from the molten droplet, but at high pressures the flame becomes contiguous to the droplet surface. Figure 5.16 shows the effect of the ambient pressure on the flame stand-off ratio, which is the ratio of the flame radius to that of the droplet. The flame and droplet radii were measured from the film during stage II, which is considered as the most stable stages during the the combustion events. The flame stand-off ratio decreases as the ambient pressure increases. This result agrees with diffusion theory which states that increases in the

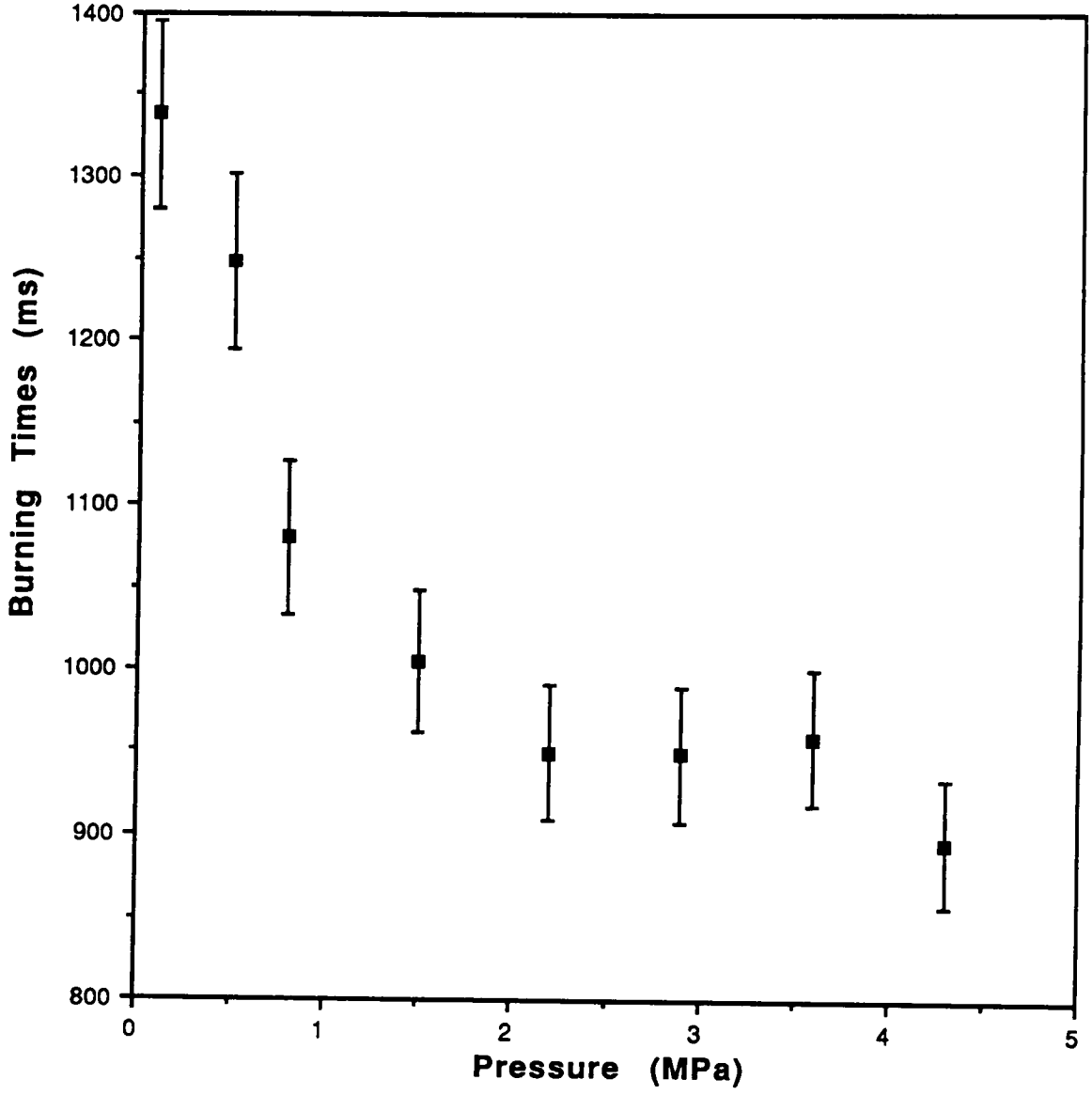

FIGURE 4.15 Effect of Pressure on the Burning Times

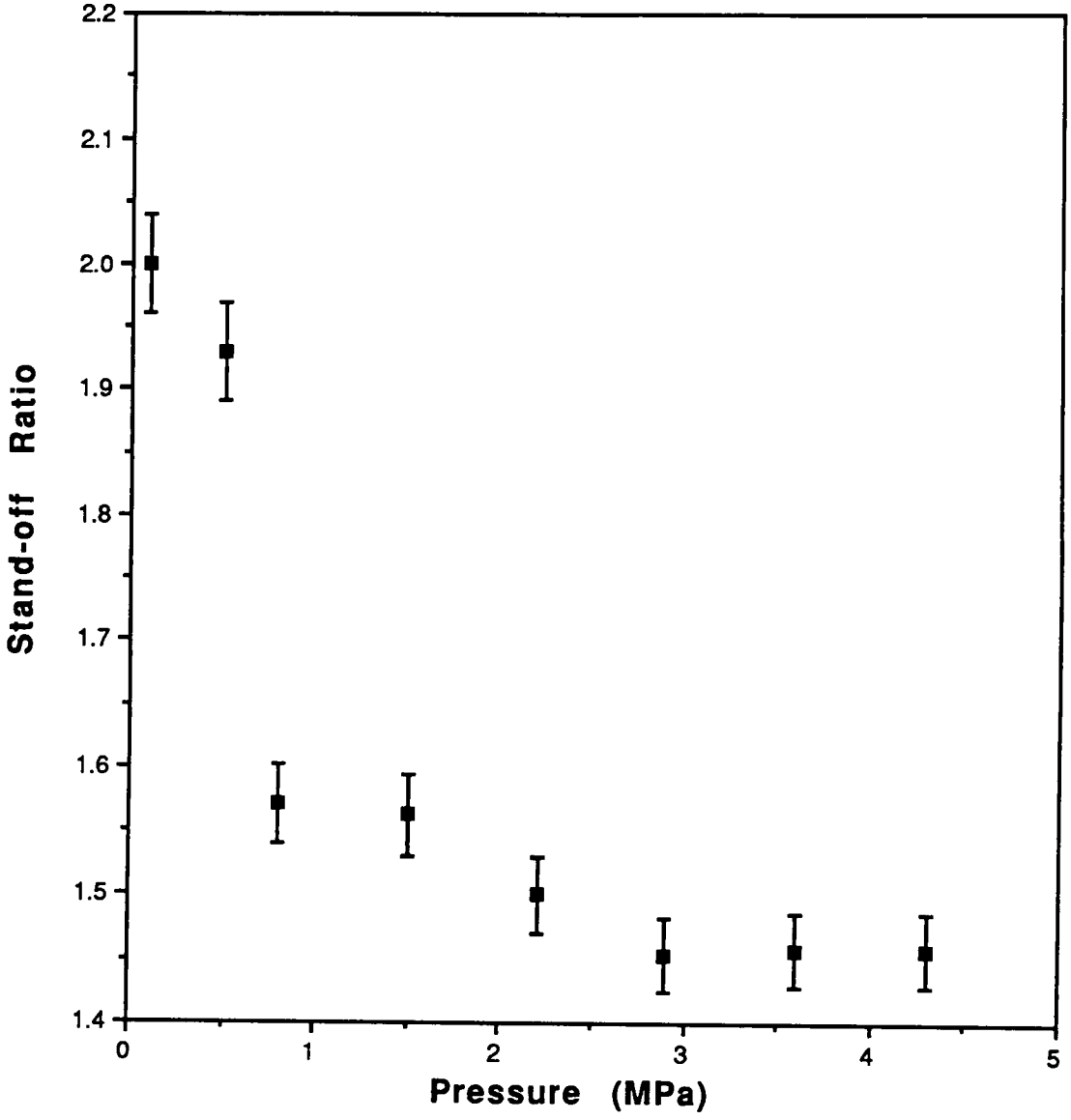

FIGURE 4.16 Effect of Pressure on the Flame Stand-off Ratio

ambient pressure are accompanied by the movement of the flame to the droplet surface. The flame structure has well-defined flame envelopes over the whole pressure range. The flame consists mainly of a white zone surrounded by a thick green envelope which is, in turn, surrounded by a thin blue-violet zone. At low pressures the molten droplet can be clearly seen through the white zone, however at high pressures the radiation emitted from the droplet increases and the droplet becomes obscured.

CHAPTER 5

CONCLUSIONS AND RECOMMENDATIONS

The objectives of the present study were to investigate the effects of pressure on the ignition time, burning time and the flame structure of aluminum agglomerates. Aluminum agglomerates of nominal diameter 535 μm were mounted in a high pressure combustion chamber and ignited using a CO_2 laser pulse. These experiments were performed in a quiescent O_2/N_2 (20/80) environment. A two-color pyrometer and a broad band radiometer were employed to measure the surface temperature and the emitted droplet radiation, respectively. A high-speed camera was also utilized to record the phenomenological events during the ignition and combustion of aluminum agglomerates.

Aluminum agglomerates do not ignite easily because of the protective aluminum oxide layer that surrounds the agglomerate. Therefore, the agglomerate temperature has to reach the melting temperature of aluminum oxide (2315 K) in order for ignition to occur. This study confirms that the ignition temperature is essentially equal to the melting temperature of aluminum oxide. The ignition delay time was found to vary between 55 and 80 ms with no obvious trend that indicates the effect of pressure as an independent parameter.

The combustion of aluminum agglomerates occurs primarily in the vapor phase. Aluminum vapor diffuses outward to react with the

oxidant in the reaction zone. The existence of the green envelope (AlO), as seen in the film record, suggests that the reaction is a multi-steps reaction which should be considered when modeling the combustion of aluminum agglomerates.

In the range of pressures investigated in this study (0.1 to 4.3 MPa), the combustion of aluminum agglomerate consists of three different stages. In the first stage, the droplet burning is steady and the flame is nearly symmetrical around the droplet. In this stage the aluminum burning is similar to that of a hydrocarbon fuel droplet with neither droplet movement nor particle fragmentation. The second stage is characterized by droplet movement and particle ejection. Strong fragmentation was observed at medium pressure range (0.8-1.5 MPa). On the other hand, sporadic and weak fragmentation was recorded at both low and high pressure regimes. In this stage the oxide accumulation affects the droplet burning mechanism. At low pressure (0.1 MPa) the oxide accumulation was actually observed on the film records as a cap at the bottom of the droplet. Furthermore, the flame symmetry becomes distorted and periodical luminosity of the droplet was observed. This suggests that the droplet was spinning while it is burning. The green envelope also increases in this stage. The last stage is characterized by the continuous decrease of the flame size and the cease of the particle fragmentation and droplet movement. Finally, the flame becomes localized on one side and then collapses of the oxide surface.

The burning time was found to decrease with increasing

ambient pressure. However, this decrease in burning time is more sensitive to pressure at low pressures than that at high pressures (where the burning time is nearly constant). Qualitative studies of the flame structure indicate that the flame consists of three different zones: an inner luminous white zone surrounded by a thick green envelope which is in turn adjoined by a thin blue-violet zone. The ambient pressure effects the flame front position. At low pressure, the flame is located away from the droplet surface. As the pressure increases the flame moves toward the droplet and at a pressure of 4.3 MPa the flame becomes contiguous to the droplet surface. The flame stand-off ratio also decreases as the pressure increases and becomes nearly constant at high pressure regime. Furthermore, an increase in ambient pressure has an effect on oxide condensation. At low pressure (0.1-0.5 MPa) most of the vapor oxide is condensed on the SiC fiber, but at high ambient pressure most of the oxide product is condensed on the surface of the aluminum droplet. In addition, this investigation has shown that an increase in the pressure also increases thermal radiation from the droplet.

From the temporal output of the pyrometer, the surface temperature curves correlated with neither the radiation intensity curves nor with the film records. This discrepancy was attributed to the upward movement of the droplet which moved out of view of the pyrometer target area. Therefore, for future study it is recommended that the size of the target area be increased in order to account for the unsteady behavior of the burning aluminum droplet.

LIST OF REFERENCES

1. Davis,A.," Solid Propellants: The Combustion of Particles Metal Ingredients," Second Rocket Propulsion Symposium, Grandfield, 1962, pp.359-367.
2. Price, E.W., "Combustion of Metalized Propellants," Progress in Astronautics and Aeronautics, AIAA, NY, Vol.90, 1983, 479.
3. Szekely,Jr., G.A., and Faeth,G.M., " Combustion Properties of Carbons Slurry Drops," AIAA Journal. Vol. 20, 1982a, 422.
4. Szekely,Jr., G.A., and Faeth,G.M., " Reaction of Carbon Black Slurry Agglomerate in Combustion Gases," 19th Symposium (International) On Combustion, The Combustion Institute, Pittsburgh, P.A.,1982b, 1077.
5. Szekely,Jr., G.A., Turns,S.R., and Faeth,G.M., " Effects of Carbon-Black Properties on the Combustion of Carbon-Black Slurry Agglomerates," Combustion and Flame, Vol 58,1984, 31.
6. Friedman, R., and Macek, A., "Ignition and Combustion of Aluminum Particles in Hot Ambient Gases," Kinetics and Combustion Division, Atlantic Research Corporation, Paper 9-19, March 1962.
7. Friedman, R., and Macek, A., "Combustion Studies of Single Aluminum Particles," 9th International Symposium on Combustion, The Combustion Institute, Pittsburgh, PA., 1963, 703.
8. Brzustowski, T. A., and Glassman, I. "Vapor-Phase Diffusion

Flames in the Combustion of Magnesium and Aluminum I: Analytical Development," Progress in Astronautics and Aeronautics, Academic Press, Vol.15, 1964, 75.

9. Bartlett, R.W., ong, Jr,J.N., Fassel, Jr., W.M., and Papp, C.A., "Estimating Aluminum Particle Combustion Kinetics," Combustion and Flame , Vol.7, 1963, 227.

10. Prentice, J.L., " Combustion of Pulse-Heated Single Particles of Aluminum and Beryllium," Combustion Science and Technology, Vol.1, 1969, pp. 385-398.

11. Wilson, R.P., Jr. and Williams, F.A., "Experimental Study of the Combustion of Single Aluminum Particles in O_2/Ar" 13th Symposium (International) on Combustion, The Combustion Institute, Pittsburgh, P.A., 1970, pp 833-845.

12. Law, C.K., "A Simplified Theoretical Model for the Vapor-Phase Combustion of Metal Particles," Combustion Science and Technology, Vol.7, 1973, 197.

13. Wong, W.G.,Turns,S.C.,"Ignition of Aluminum Slurry Droplets" Combustion Science and Technology, Vol.52, 1987, 221

14. Turns,S.C., Wong,W.g. and Rbya,E., "Combustion of Aluminum-Based Slurry Agglomerates," Combustion Science and Technology, Vol.54, 1987, 299.

15. Schechter, C.B., "An Experimental Investigation of the Ignition and Combustion Phenomena of Laser-Ignited Boron Agglomerates in a Flowing Oxygen Environment," Master's

Thesis, University of Tennessee, 1990.

16. Holman, J.P., "Experimental Methods for Engineers," 4th Edition, McGraw-Hill Book Company, New York, 1984, 59.
17. Zaidi, W.H.S., "Ignition and Combustion Phenomena of Laser-Ignited Boron Agglomerates at Elevated Pressures," Master's Thesis, University of Tennessee, 1991.
18. Rautenberg, T.H., Jr., and Johnson, P.D., "Light Production in the Aluminum-Oxygen Reaction," J. Opt. Soc. Amer, Vol.50, 1960, 602
19. Brzustowski, T.A, and Glassman, I., "Spectroscopic Investigation of Metal Combustion," Progress in Astronautics and Aeronautics, Academic Press, Vol.15, 1964, 41.
20. King, M.K.," Ignition and Combustion of Boron Particles and Clouds,"AIAA Journal, Vol. 19, 1982, 294.

VITA

Khaled Meftah was born in Kairouan, Tunisia on April 17, 1966. He graduated from Al-Mansoura High School in June 1986. Meftah was awarded a scholarship by the Tunisian Government to study in the U.S. He entered the University of Tennessee, Knoxville in the spring 1987. He received the bachelor degree in Mechanical Engineering with high honors in August of 1990. He continued his study at the University of Tennessee, Knoxville where he received his Master of Science Degree in Mechanical Engineering in May of 1992.